Long-term Variability and Trends of Agulhas Leakage and its Impacts on the Global Overturning

Hendrik Großelindemann[1,3], Frederic S. Castruccio[2], Gokhan Danabasoglu[2], and Arne Biastoch[1,3]

[1]GEOMAR Helmholtz Centre for Ocean Research Kiel, Kiel, Germany
[2]US National Science Foundation National Center for Atmospheric Research, Boulder, CO, USA
[3]Christian-Albrechts Universität zu Kiel, Kiel, Germany

Correspondence: Hendrik Großelindemann (hgrosselindemann@gmail.com)

Abstract. Agulhas leakage transports relatively warm and salty Indian Ocean waters into the Atlantic Ocean and as such is an important component of the global ocean circulation. These waters are part of the upper limb of the Atlantic Meridional Overturning Circulation (AMOC), and Agulhas leakage variability has been linked to AMOC variability. Agulhas leakage is expected to increase under a warming climate due to a southward shift in the South Hemisphere westerlies, which could further
5 influence the AMOC dynamics. This study uses a set of high-resolution pre-industrial control and historical and transient simulations with the Community Earth System Model (CESM) with a nominal horizontal resolution of $0.1°$ for the ocean and sea-ice and $0.25°$ for the atmosphere and land. At these resolutions, the model represents the necessary scales to investigate the Agulhas leakage transport variability and its relation to the AMOC. The simulated Agulhas leakage transport of $19.7 \pm 3\,Sv$ lies well within the observed range of $21.3 \pm 4.7\,Sv$. A positive correlation between the Agulhas Current and the Agulhas
10 leakage is shown, meaning that an increase of the Agulhas Current transport leads to an increase in Agulhas leakage. The Agulhas leakage impacts the strength of the AMOC through Rossby wave dynamics that alter the cross-basin geostrophic balance with a time-lag of 2-3 years. Furthermore, the salt transport associated with the Agulhas leakage influences AMOC dynamics through the salt-advection feedback by reducing the AMOC's freshwater transport at 34°S. The Agulhas leakage transport indeed increases under a warming climate due to strengthened and southward shifting winds. In contrast, the Agulhas
15 Current transport decreases, both due to a decrease in the Indonesian Throughflow as well as the strength of the wind-driven subtropical gyre. The increase in Agulhas leakage is accompanied by a higher salt transport into the Atlantic Ocean, which could play a role in the stability of the AMOC by the salt-advection-feedback.

1 Introduction

Agulhas leakage is part of a current system around South Africa which connects the Atlantic Ocean to the Indian Ocean
20 and is an important component for the global ocean circulation. Warm water from the Indian Ocean flows southward along the coast of South Africa as a western boundary current, the Agulhas Current, until it detaches from the coast and reaches a region of strong westerly winds (Figure 1). The dynamics of the flow then become an interplay between its southward inertia and the wind forcing (Beal et al., 2011): The winds push most of the water back eastwards into the Indian Ocean which is called the Agulhas Retroflection. However, some part of the water leaks into the Atlantic Ocean due to instabilities and non-

25 linear dynamics. Prominent mesoscale rings form, the so-called Agulhas Rings, and propagate north-westwards carrying the relatively warm and salty waters of the Indian Ocean into the South Atlantic. This transport of heat and salt into the upper Atlantic Ocean plays a role in the Atlantic Meridional Overturning Circulation (AMOC) and subsequently the global conveyor belt (Schulzki et al., 2024).
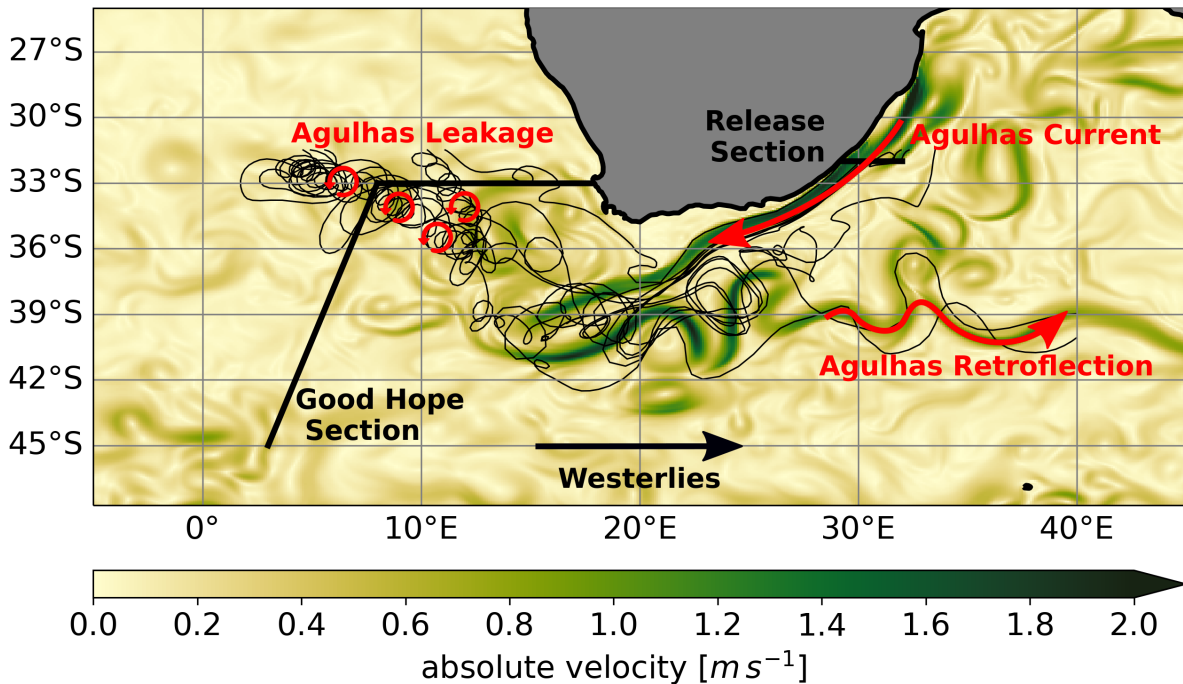
Figure 1. Map of the Agulhas region; colours show a snapshot of the five-daily mean velocity magnitude field from the FOSI simulation, thin black lines are example tracks of Lagrangian particles, thick black lines show the release and crossing section and red arrows schematically represent the circulation features.

The trade winds in the Indian and Atlantic Ocean together with the strong westerlies in the Southern Hemisphere form sub-
30 tropical gyres in each basin. Because the African continent does not cross the mean position of the zero line of the wind stress curl, both systems are connected and can be described as one supergyre (Speich et al., 2007). The Agulhas system shapes this connection and therefore opens up a pathway between both ocean basins. The amount of trans-basin transport is controlled by the wind field (Beal et al., 2011). The winds over the Indian ocean determine the inertia of the Agulhas Current, which together with the strength of the westerlies, controls whether the current turns west into the Atlantic or loops back into the Indian Ocean.
35 Ultimately, it is this interplay between the two that controls how much water is leaking into the Atlantic (Durgadoo et al., 2013). Rühs et al. (2022) found that an increase in the wind stress curl over the Indian Ocean resulting from strengthened winds leads to an increase in the Agulhas leakage.

Agulhas leakage is not a straight current that flows into the Atlantic Ocean, but rather consists of mesoscale rings, which form in the retroflection region and then propagate into the Atlantic (Olson and Evans, 1986). These Agulhas Rings are affected by the bathymetry and take different routes into the basin, some even reaching the Brazilian coast (Dencausse et al., 2010). The formation rates and propagation speeds of these rings lead to variability in the overall transport on interdecadal timescales (Holton et al., 2017). They have an average radius of $150 - 200\,km$, about $5 - 6$ rings form per year and then propagate into the Atlantic at a speed of $5 - 15\,km/day$ (Schouten et al., 2000). The eddy activity is additionally impacted by large scale climate modes such as the Southern Annular Mode or the El-Nino Southern Oscillation (Morrow et al., 2010). Another but not as important pathway for Indian Ocean waters is the Good Hope Jet, described as an extension of the Agulhas Current along the continental slope (Gordon et al., 1995).

Relatively warm and salty surface waters from the Indian Ocean are transported into the Atlantic by Agulhas leakage, and connect to the upper part of the AMOC as part of the "warm-water route" of the global overturning circulation in the Atlantic Ocean (Gordon, 1986; Rühs et al., 2019). It is hypothesized that these water properties influence the formation of deep water in the North Atlantic mainly through the salt input. Weijer and van Sebille (2014) investigated the influence of salinity input of Agulhas leakage into the Atlantic on the AMOC on interdecadal timescales. While they could show an advective connection from Agulhas leakage to the North Atlantic, no impact to the AMOC strength could be detected. However, due to a bias in salinity in the model, the salinity anomalies induced by the Agulhas leakage were much weaker than in the observations. Biastoch et al. (2008) showed the influence of the Agulhas leakage, in this case through Rossby and topographic shelf waves, on AMOC variability on decadal timescales is on the same order as that of deep water formation in the North Atlantic. Another study by Biastoch et al. (2015) found that the Atlantic multi-decadal variability (AMV), a basin-wide North Atlantic sea surface temperature fluctuation on multi-decadal time scales, covaries with Agulhas leakage. Still, the exact relationship between the Agulhas leakage and the AMOC is not that clear, both for the volume transport as well as for the hydrographic influences.

The stability of the AMOC and hence the possibility of a future collapse is a major topic in current research (Boulton et al., 2014; Hu et al., 2021; Boers, 2021). A major theory involved here is the salt-advection feedback. It describes the AMOC stability as a feedback loop between the AMOC strength in the North Atlantic which controls the freshwater transport through 34°S, which influences the density difference between the North and the South Atlantic which then again influences the AMOC strength. The direction of the freshwater transport, either southward or northward, determines the sign of the feedback loop being positive or negative, respectively. More precisely, a negative feedback loop describes a self-stabilising system; an AMOC change is balanced by the other components which then revert the change back to its original state. A positive loop however describes the opposite; an AMOC weakening f.e. is enhanced by the other components which further increases the weakening and leads to an unstable system. The process originates from a theory by Stommel (1961) based on simple box models and was further developed by Rahmstorf (1996). A negative freshwater transport describes a bi- or multi-stable AMOC where a sudden shift in the freshwater forcing can lead to an AMOC collapse (Rahmstorf, 1996; Van Westen et al., 2024; Lohmann et al., 2024). Observations of the real ocean estimate a negative freshwater transport (Arumí-Planas et al., 2024). Climate models exhibit the full range of values while a positive value can also be part of a bi-stable AMOC regime in some models (Van Westen and

Dijkstra, 2024). The impact of the Agulhas leakage on this freshwater transport and further impacts on the AMOC remain to be completely understood (Weijer et al., 2019).

Furthermore, the Indian Ocean Throughflow (ITF), a connection between the Pacific and the Indian Ocean, has an impact on Agulhas leakage. Bars et al. (2013) and Makarim et al. (2019) showed that the ITF influences the strength of the Agulhas Current and subsequently Agulhas leakage. Van Sebille et al. (2009) have shown that an increase in the Agulhas Current strength leads to a decrease in Agulhas leakage due to higher inertia of the Agulhas Current and therefore stronger retroflection. However, this result has been under discussion since then and Loveday et al. (2014) describe a decoupling of the Agulhas leakage strength from Agulhas Current variability. Zhang et al. (2023) found variability in the Agulhas Current on decadal and multi-decadal timescales, which might impact Agulhas leakage depending on the exact relation between them. This highlights the complexity of the region and how many factors can play a role in determining the strength of Agulhas leakage.

It is projected and already observed, that the Southern Hemisphere westerlies are strengthening and moving southward under climate change (Cai, 2006). This has direct impacts on the controlling dynamics of the Agulhas leakage. Biastoch et al. (2009) related the southward shift to an increase in leakage and by that a salinification of the South Atlantic. A modelling study by Beech et al. (2022) shows an increase in eddy activity in the region and a connected increase in Agulhas leakage by up to 6 Sv due to climate change. Additionally, Ivanciu et al. (2022) used a high-resolution nesting approach as well as interactive ozone forcing to show that Agulhas leakage is increasing by 1.5 Sv over 80 years. A recent study by Li et al. (2022) highlights the importance of a poleward shift of mid-latitude easterlies globally in controlling the southern boundary of subtropical ocean gyres and subsequently the southward extent of western boundary currents.

Due to the fact that mesoscale dynamics are highly important in the Agulhas region and especially in Agulhas leakage, these processes need to be resolved to capture the Agulhas leakage transport (Schubert et al., 2021). Over the past decade, growth in ocean modelling capabilities allowed for eddy-resolving resolutions, i.e. grid sizes smaller than the local Rossby deformation radius, in the Agulhas region and therefore its investigation. However, these were mainly hindcast simulations covering around 60 years from 1960 to 2020, which limits the modes of variability that one is able to extract. Little is known about the variability of the system on timescales of decades to centuries (Beal et al., 2011; Rühs et al., 2022). In order to investigate this, high-resolution and multi-centennial model configurations are needed. The model used for this study is a high-resolution configuration of the Community Earth System Model (CESM) which consists of a 0.1° ocean and therefore resolves mesoscale processes (Chang et al., 2020). The global high-resolution is particularly important to better represent the global overturning circulation (Roberts et al., 2020). The available high-resolution CESM simulations include a 500-year pre-industrial control (PIcontrol) run and a 3-member ensemble of historical and transient simulations in which the transient (future projection) period uses the Representative Concentration Pathway 8.5 (RCP8.5). These offer a unique opportunity to examine Agulhas leakage variability on timescales of decades and longer, allowing an assessment of possible changes in Agulhas leakage in a warming climate. Additionally, one can investigate the connection of Agulhas leakage to the global climate in a self-consistent, fully coupled Earth System Model as opposed to forced regional ocean-only simulations.

This study is structured as follows: We first describe the model and simulations, then explain how we estimate Agulhas leakage transport with a particle tracking algorithm and the applied analysis methods. We then investigate the following ques-

tions: What is the internal variability of Agulhas leakage on decadal to multi-decadal timescales and what are related driving mechanisms? How is Agulhas leakage connected to the global overturning circulation and specifically the AMOC? And how might the system change in a warming climate? We end with discussing the results with existing literature and concluding our findings.

2 Model and simulations

This study uses the high-resolution version of the Community Earth System Model (CESM-HR; Chang et al. (2020)). CESM-HR is based on an earlier model version, CESM1.3, as described in Meehl et al. (2019) with many additional modifications and improvements over its standard version. The ocean component is the Parallel Ocean Program version 2 (POP2 ; Danabasoglu et al. (2012); Smith et al. (2010)) with a 0.1° horizontal mesh and 62 vertical levels of increasing layer thickness to the bottom. The atmosphere component is the Community Atmosphere Model version 5 (CAM5 ; Neale et al. (2012)) and has a horizontal resolution of 0.25° and 30 vertical levels. The other components are the Community Ice Code version 4 (CICE4; Hunke and Lipscomb (2008)) and the Community Land Model version 4 (CLM4 ; Lawrence et al. (2011)) with resolutions of 0.1° and 0.25°, respectively. With this configuration, a 520-year pre-industrial control run was performed. In our study, we use model years 150 to 520, avoiding the initial spin up period. Figure 2 shows all used configurations, their time periods and forcing types.
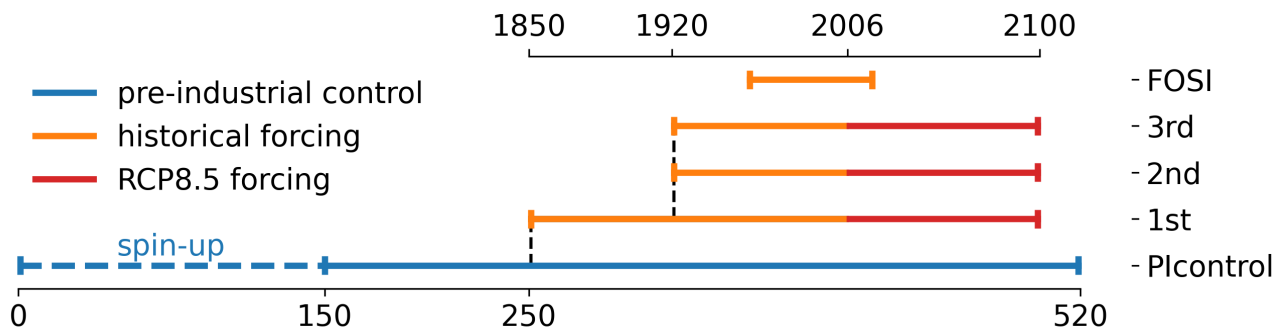
Figure 2. Schematic of the CESM simulations used in the manuscript; the PIcontrol and the three ensemble members use the fully-coupled CESM while FOSI represents a Forced Ocean - Sea Ice simulation using the same CESM ocean and sea-ice models. Colours indicate different CO_2-forcing types and the black dashed lines show branching of another run.

It has been shown that this simulation captures many features of the current climate well, showing improvements compared to a lower resolution counterpart (1°) (Chang et al., 2020). With the same configuration, three ensemble runs were performed applying a transient CO_2-forcing to simulate climate change. The first member was branched from PIcontrol at model year 250 or calendar year 1850. The second and third members were branched from the first member at year 1920, because the first 70 years contain little forcing, saving computing time. Historically observed CO_2 forcing was applied until the year 2006 and then the RCP8.5 scenario (Van Vuuren et al., 2011) was used until 2100. Additionally, we use output from a forced ocean-sea

ice (FOSI) hindcast simulation for the 1958-2018 period. FOSI employs the same ocean and sea-ice components, forced with the JRA55-do dataset from Tsujino et al. (2018).

130   We use satellite based dynamic sea level (Sea Surface Height above geoid) daily means from 1993 to 2018 to evaluate the model's capability to resolve the necessary mesoscale activity in the region and the overall large scale circulation pattern. These data are provided by the Copernicus Marine Environment Monitoring Service (CMEMS) on a global grid of 0.25° resolution and are based on a data unification and altimeter combination system (Mertz et al., 2017).

3   Methods

135   ### 3.1   Agulhas leakage Estimation

To calculate annual Agulhas leakage transport, we follow a well-established methodology by Schmidt et al. (2021); Rühs et al. (2022). We perform a Lagrangian particle tracking method, utilising the python package Oceanparcels (Delandmeter and Van Sebille, 2019; Kehl et al., 2023). Directly tracking particles to infer their pathway relies on a good representation of the prevailing velocity field. Due to the high mesoscale activity in the region, eddy-resolving resolutions (<=1/10°) are therefore

140   necessary to apply this method for a meaningful transport estimation (Schmidt et al., 2021). Particles are released every month of the model output along a section at 32°S from 29-32°E through which the Agulhas Current flows southward along the coast of South Africa (Figure 1). An initial transport is assigned to each particle, based on the volume around them and the velocity at that point and then tracked for five years. The tracking is an interpolation that applies a fourth-order Runge-Kutta advection scheme (Delandmeter and Van Sebille, 2019). We use an internal timestep of 32 minutes for the advection scheme, based on

145   the grid size of the model. This timestep keeps the particles in the same grid box for at least two timesteps with still reasonable computational effort. The annual total Agulhas leakage transport then consists of the volume of all particles that cross the Good Hope section as their first exit from the domain during a five year tracking period. Observations have been done along the Good Hope section since 2004, including conductivity-temperature-depth profiles and mooring deployments, and it is part of the South Atlantic observing network of the meridional overturning circulation (Speich et al., 2023). Because the majority

150   of particles cross the section in the first year (Van Sebille et al., 2018), the whole transport of five years is assigned to the release year. Ideally, this tracking is performed on the full 3D velocity field and on a high, daily to 5-daily, temporal output of an ocean model. However, the 3D fields were only available in monthly resolution for the coupled simulations. We therefore tested different techniques using different fields and temporal resolutions to find the best possible estimate we could get from the PIcontrol. Figure A1 shows decadally-filtered timeseries (see Section 3.2 for filtering method) of all used approaches for

155   Agulhas leakage calculation. This effort includes 3D tracking on five-daily and monthly velocity fields, as well as a regression method based on horizontal geostrophic velocities calculated from the Dynamic Sea Level (DSL). This regression method was developed and validated by Rühs et al. (2022). We tested the regression in the FOSI simulations, where the five-daily 3D velocity field for the 1983-2015 period was available. This FOSI analysis gives us an estimate of Agulhas leakage at high temporal resolution. The regression between the 3D (red line) and the geostrophic surface tracking and then applied to

160   reconstruct the total Agulhas leakage transport from the surface tracking (purple line) leads to good alignment between both

with a significant correlation of 0.92 based on a 95% level, exceeding a correlation of 0.86 from Rühs et al. (2022). This indicates that this regression is a valid technique of reconstructing the Agulhas leakage transport, when only surface velocities are available.

In order to find the longest possible, but also plausible timeseries of Agulhas leakage in the PIcontrol, we compare the estimated transport from the available fields based on their correlation and variances (Figure A1). Plausibility is however not easy to determine since differences can be based on true signals in the circulation we want to sample, but also on errors from the particle tracking e.g. due to lower temporal resolution. We had 370 years of monthly 3D velocity and DSL data from year 150 to 520 and five daily DSL data from year 338 to 512. Therefore, we had to decide between completely relying on the fully-coupled system or combining the DSL tracking with the regression from the more precise FOSI simulation to get a full transport estimate. We applied the regression on the 174 years of five-daily DSL tracking as our best estimate for high temporal resolution in the PIcontrol (blue line). Then, we compared this timeseries to the 370 years of monthly data, both for the full 3D tracking (green line) and the DSL tracking with the regression applied (yellow line). We found significant correlations of 0.77 between the five daily DSL and the monthly 3D tracking, while it was only 0.59 between five daily and monthly DSL. On decadally-filtered timeseries, we found a significant correlation of 0.82 between the five-daily DSL and the monthly 3D. For the monthly DSL tracking, the correlation was less with 0.69 and just not significant with a p-value of 0.06. Regarding the interannual variation of the transport expressed as a standard deviation, a value of 2.48 Sv from the five-daily 3D tracking of FOSI is our best estimate, i.e., *truth*. In PIcontrol, the standard deviations are 2.85 Sv and 3.01 Sv for the monthly DSL and 3D tracking, respectively, which are both larger than, but close to the true value.

We decided to use the monthly 3D tracking method to obtain a 370-year timeseries of the Agulhas leakage transport because of better correlations and standard deviations of interanually- and decadally-filtered data with the truth than those of the DSL approach. However, the volume transport from the particle tracking can vary depending on the release section. Schmidt et al. (2021) show an increase of $2\,Sv$ from a release at $32°$ S (as we do) to a release at the ACT (Agulhas Current Time-Series) section at $34°$ S, where the observational estimates from Beal et al. (2015) and Daher et al. (2020) are based on. On the other hand, using monthly data instead of a higher temporal resolution can lead to a more laminar flow with tracking and an associated increase in the volume transport. We found an increase of around $2\,Sv$ due to this in FOSI (red and brown lines in Figure A1). Both factors, the different release sections and the bias due to the different temporal resolutions, could even out, but we cannot quantify these impacts. Because our focus is on decadal and longer variability, the calculation based on monthly 3D velocities is an appropriate strategy. This is confirmed by Cheng et al. (2016), who showed that monthly mean outputs are sufficient to investigate variability on time scales longer than seasonal. Additionally, the 3D tracking allows us to track the temperature and salinity along a particle's trajectory, which we can use for further analysis. We define the Agulhas Current transport as the sum of the transport of all released particles. This is different than just calculating the volume transport through a section, because we are only releasing particles at points that have a southward velocity, e.g., into the domain.

3.2 Analysis

To evaluate the representation of the ocean circulation around South Africa in our simulations, we first compare simulated and satellite-based Dynamic Sea Level variability. We use the first ensemble member of the CESM transient simulations and the overlapping period from 1993 to 2018 to be most consistent with the observations and calculate their standard deviations. Additionally, observational transport estimates based on floats and drifters for the Agulhas leakage (Daher et al., 2020) as well as mooring data for the Agulhas Current (Beal et al., 2015) are compared to the results of the particle tracking.

To investigate variability of Agulhas leakage on different timescales, we perform a spectral analysis using the annual-mean timeseries. Due to the relatively short length of this timeseries data, meaning only 370 data points, this was not a straightforward exercise. We employ just a general Fourier Transform and not a wavelet analysis to better resolve the longer frequencies. The significance of the peaks is calculated following Torrence and Compo (1998). In general, significance in this study always refers to the 95% level. To explore relationships between two timeseries, we perform lead-lag correlation analysis. For these, the data have been filtered using a five-year Hanning window and are detrended. Significance is based on a two-sided student's t-test, that incorporates the autocorrelation of each timeseries. We perform coherence analysis to investigate co-variability between two timeseries and infer possible driving mechanisms. Because the results of the coherence analysis are quite dependent on the window size for the wavelets, we calculate coherence over a range of sizes with zero padding for the smaller ones to keep the same frequency resolution. Then, we average the coherence distributions of all window sizes to get the dominant frequencies. The confidence levels are estimated following Thompson (1979) and are averaged in the same way.

We extract wind metrics as the maximum and minimum zonal wind stress in the region between 20°E to 110°E and 20°S to 60°S, following Rühs et al. (2022). The maximum and minimum zonal wind stress represent the Southern Hemisphere Westerlies and the Subtropical Easterlies, respectively. This then also gives us their latitude and thereby their position. Additionally, we calculate the average wind stress curl in the same longitudinal range, but between 35°S and 45°S. The regions can be seen in Figure A2. The Southern Annular Mode is defined as the first Empirical Orthogonal Function (EOF) mode of the annual-mean sea-level pressure south of 20°S and it is calculated using the Climate Variability Diagnostics Package package (CVDP) (Phillips et al., 2014; Thompson and Wallace, 2000).

Because salinity of each particle along its trajectory is tracked, it is possible to calculate the salt transport of Agulhas leakage, F_S, into the Atlantic Ocean. This has been calculated following the method from Weijer and van Sebille (2014), where the amount of salt, that a particle brings into the Atlantic, is the difference of its salinity S_i at the Good Hope Section and the long-term salinity mean $\overline{S}$ (at the crossing location along the section and at the same depth) times its transport V_i and then sum up all particles that cross the Good Hope section:

$$F_S(t) = \Sigma_i V_i(t)(S_i(t) - \overline{S})$$

where t is time. Therefore, by referring to the average salinity at the section, salt transport variations are the advection of local salinity anomalies only. Variations in the volume transport alone would not cause any variance in the salt transport (Weijer and van Sebille, 2014). However, as there is a small salinity drift in PIcontrol, i.e., a freshening over time, we use a linear fit of the section mean over time instead of just the temporal mean. For the transient simulations, the reference salinity was a constant

temporal mean from 1920-2100 to allow for a potential trend in the salt transport that is based on climate change and not on a model drift. Additionally, we only choose particles between $150\,m$ and $1500\,m$ to remove mixed layer influences, being consistent with Weijer and van Sebille (2014).

230   To investigate the impact of the Agulhas leakage onto the AMOC, we compute AMOC transports at different latitudes. The AMOC strength is the maximum value of the AMOC stream function in depth space and deeper than 500 m, excluding the surface cells. Additionally, we investigate a relation between the Agulhas leakage salt transport and the freshwater transport induced by the overturning circulation at 34°S. We use the method described in Jüling et al. (2021) to calculate the annual freshwater transport F_{ov}:

235
$$F_{ov} = -\frac{1}{S_0} \int (\int\limits_{W}^{E} v^* dx)(\langle S \rangle - S_0) dz$$

where $S_0 = 35\,psu$, $\langle S \rangle$ is the zonal-mean salinity, and $v^* = v - \hat{v}$ with $\hat{v}$ being the section-mean meridional velocity. This freshwater transport is thought to be an important aspect of the salt-advection feedback contributing to AMOC stability.

    The ITF is another important pathway for the global overturning and can be used to investigate its connections and changes (Durgadoo et al., 2017). To estimate the ITF volume transport, we calculate the annual-mean transport through sections cover-

240 ing each strait from the Pacific to the Indian Ocean between Thailand and Australia and sum up the sections. We estimate the wind-driven part of the Agulhas Current as the Sverdrup transport at 32°S in order to separate wind-driven from the overturning circulation. This transport is calculated following the formula from Sverdrup (1947).

    When investigating future changes, we take the ensemble mean from the three ensemble members for their overlapping period from 1920 to 2100. While three ensemble members are not that many, it removes some of the internal variability and

245 therefore increases the robustness of examined trends due to global warming.

4   Results

4.1   Model representation of the region

To determine the fidelity of our CESM simulations in resolving the necessary dynamics in our region of interest, we compare the Dynamic Sea Level variability from the PIcontrol simulation to that of satellite observations in Figure 3. The strongest

250 variability in the observations appears around 20°E and 40°S. This is where the Agulhas Current reacts to the overlying wind field and is being pushed back to the East. Upstream of this location, the Agulhas Current is rather stable, leading to a corridor of low variability. The higher variability around Madagascar is due to mesoscale eddies as well, the eddies then feed into the Agulhas Current. The flow back into the Indian Ocean through the Agulhas retroflection is characterised by a meandering flow, which is visible in the Dynamic Sea Level between 35°- 40°S. Agulhas leakage itself consists mostly of large scale rings, that

255 then propagate into the Atlantic, marked by the increased variability in that direction. In the model, the general picture is very similar, meaning that the model represents these observed characteristics well. However, some differences exist as well: the

variability around 20°E is stronger in the model and there is a more pronounced eddy corridor into the Atlantic Ocean. This is a known model deficiency present in simulations with other air-sea coupled models as well (Ivanciu et al., 2022).
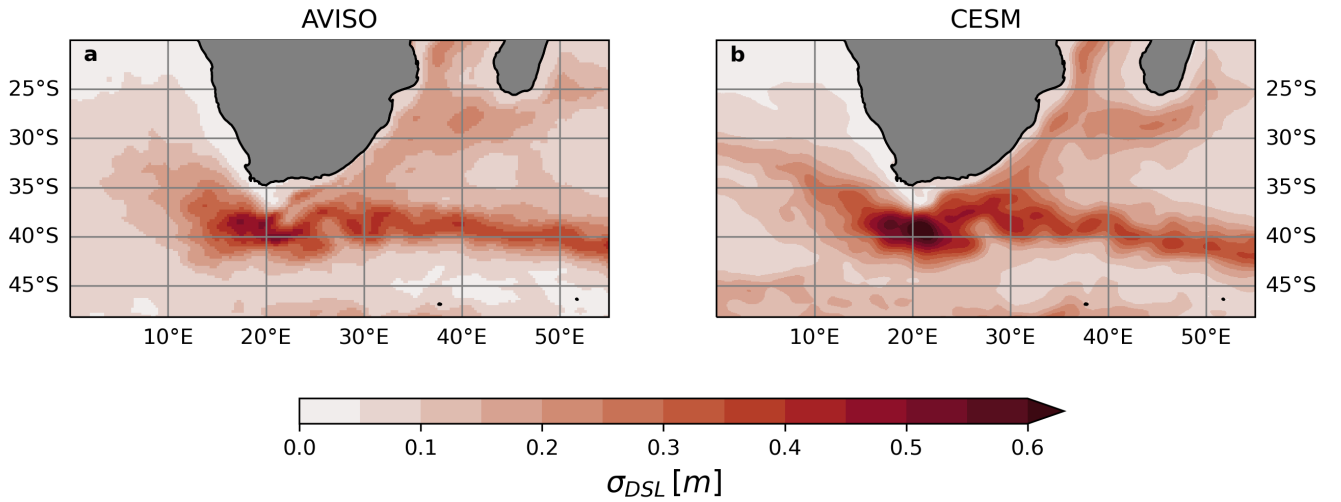
Figure 3. Dynamic Sea Level variability σ_{DSL} from daily AVISO satellite altimetry (a) and in the first ensemble member of CESM (b) for the overlapping time period from 1993 to 2018.

Our 370-year long Agulhas leakage timeseries shown in Figure 4a shows a transport of $19.7 \pm 3\,Sv$, which lies well within the most current observational estimate of $21.3 \pm 4.7\,Sv$ based on floats, drifters, and a mooring array from Daher et al. (2020) with the caveat that the simulated and observed estimates have slightly different initialization latitudes which can result in slight differences in the total transports (Schmidt et al., 2021). The simulated Agulhas Current transport of $72 \pm 4\,Sv$ is also similar to the observed transport of $77 \pm 4.0\,Sv$ from mooring data (Beal et al., 2015). We compute the ratios of Agulhas leakage transport to the Agulhas Current transport as $27.3 \pm 4\,\%$ for the model and $27.6 \pm 2.5\,\%$ for observations. Additionally and as a metric for the global overturning circulation, we find a mean AMOC transport at 26.5°N of $18.26 \pm 1.08\,Sv$ which is in the range of the RAPID array observations of $17.55 \pm 2.88\,Sv$ (Moat et al., 2023; CMEMS, 2023). Thus, these rather good agreements with observations give us additional confidence in our model's fidelity.

4.2 Variability on different timescales

The Agulhas leakage timeseries from PIcontrol shows a strong interannual variability, while the decadally-filtered timeseries hints at variability on longer timescales. The spectrum of the annual-mean timeseries presented in Figure 4b shows that the interannual variability with a period of two years clearly stands out, which is related to the formation and propagation of Agulhas Rings (Holton et al., 2017). Another significant peak is seen at a 14-year period and there are peaks also around 40-50 years, but these latter peaks are just below our significance level. To assess the robustness of these peaks, we also performed
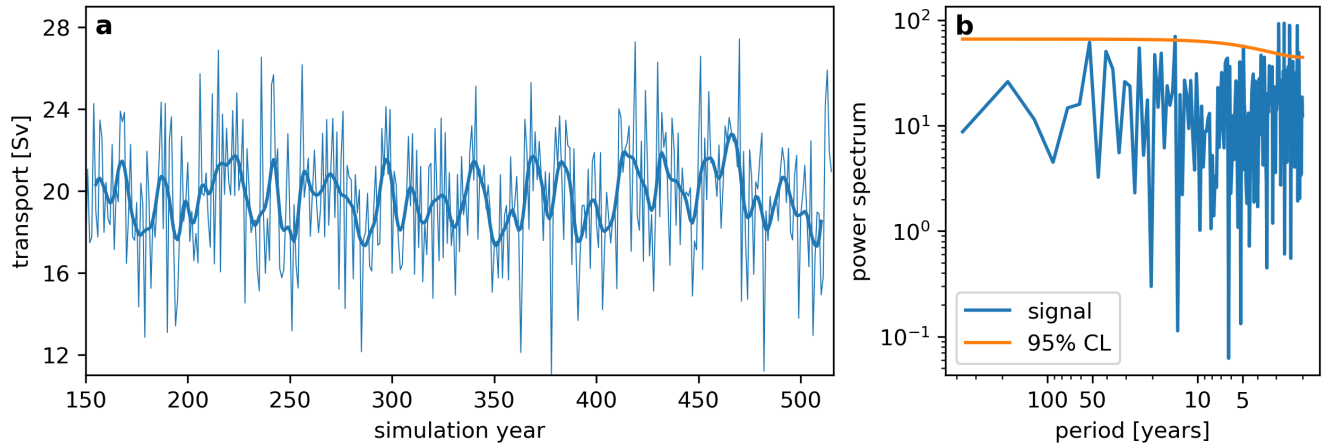
Figure 4. Agulhas leakage timeseries from the Lagrangian particle tracking for PIcontrol (a). The thin and thick lines represent annual-mean and 11-year running-mean timeseries, respectively. The power spectrum of the annual-mean Agulhas leakage timeseries (b) with the orange line showing the 95% confidence level.

spectral analysis using different estimates of Agulhas leakage (not shown). These further analyses indicate that the dominant peaks / frequencies vary considerably and that there is really no robust long-term variability peak that can be identified.

4.3 Wind forcing across scales

It is known that Agulhas leakage is driven by the prevailing wind field over the Agulhas region and the southern Indian Ocean (Beal et al., 2011). We investigate this relationship in the PIcontrol as another proof of concept before looking at longer periods, also exploring the associated timescales.

Performing a lead-lag correlation analysis shown in Figure 5a, we find that both the maximum and minimum zonal wind stress as well as the average wind stress curl over the Indian Ocean show significant lead times of 3-4 years over the Agulhas leakage. The correlation values are 0.33, 0.25 and -0.20 for the wind stress curl and the maximum/minimum zonal wind stress, respectively. These are not that high due to the strong interannual variability of the Agulhas leakage, but still significant because of the length of the timeseries. The lead time of three years relates to a Sverdrup response over the Indian Ocean, that takes some time to propagate into the region (DiNezio et al., 2009). When calculating the correlations for each point in space, presented in Figure A3, we find the strongest correlations around 50°S and 50°E. This co-locates with the maximum long-term mean zonal windstress, which means that it is indeed a strengthening of the winds that increases the Agulhas leakage and not a latitudinal shift. Additionally, we find a significant negative correlations at around 30°S and across the Indian Ocean, which is related to strengthened trade winds and hence a stronger subtropical gyre. Barotropic and baroclinic adjustment processes as well as filtering of the timeseries can explain the 0-3-year spread in the range of lead times (Anderson and Killworth, 1977).
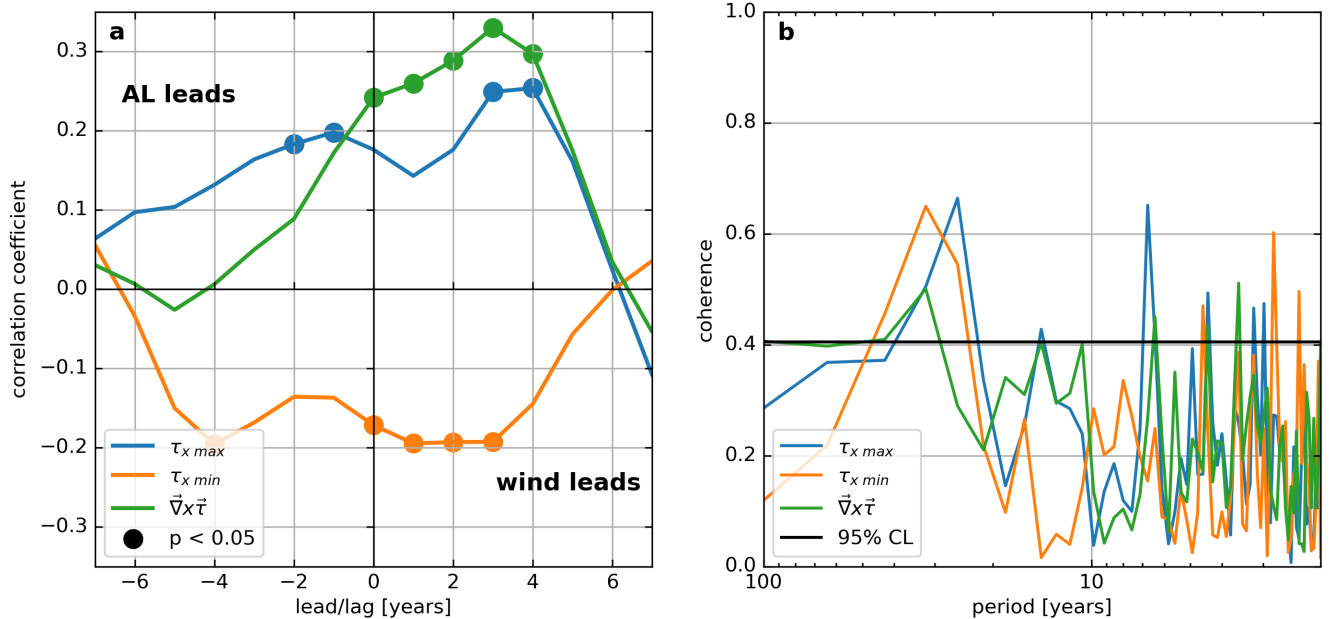
Figure 5. Lead-lag correlation (a) and coherence (b) between Agulhas leakage and the prevailing winds, in particular the maximum/minimum zonal windstress, $\tau_{x\,max/min}$, within 20°-110°E and 20°-60°S and the average windstress curl, $\mathbf{\nabla} \times \boldsymbol{\tau}$, over 20°-110°E and 35°-45°S. Significance levels are represented with the dots in (a) and the horizontal line in (b).

The coherence analysis shown in Figure 5b shows strong and significant coherence values of up to 0.66 at different periods including long-term co-variability at 14- and 30-year cycles. The wind metrics, especially the maximum zonal wind stress and the wind stress curl, have very similar coherence spectra, underlining the wind influence and suggesting that the wind is the dominant driver of Agulhas leakage across timescales.

4.4 Connection to local and global circulation

The connection of the Agulhas Current transport to the strength of the Agulhas leakage has been under discussion in the past. We calculated the lead-lag relationship between both in the PIcontrol in Figure 6. A positive and significant correlation of 0.19 stands out at zero lag. This means that a stronger Agulhas Current directly leads to a stronger Agulhas leakage in the same year. The fact that the highest correlation occurs at zero lag is reasonable because we assign the Agulhas leakage transport to the release year of the particles within the Agulhas Current.

Further into the large-scale circulation of the Atlantic, we find a significant correlation of 0.22 when the Agulhas leakage transport leads AMOC at 34°S by 2-3 years. As the majority of the particles reach the Good Hope section at 34°S within one year, this multi-year time lag of the correlation does not fit an advective timescale. However, it can be explained by invoking westward propagating Rossby waves which modify the east-west geostrophic gradient. An indicator of these waves is the depth anomaly of the 10°C isotherm (Olson and Evans, 1986) as presented in Figure A4. The figure shows a westward propagation
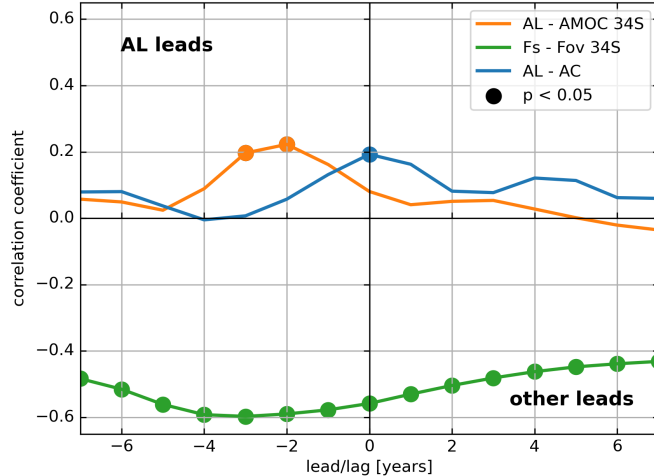
Figure 6. Lead-lag correlations between the Agulhas leakage and the Agulhas Current (AC) and the AMOC strength at 34°S as well as between Agulhas leakage salt transport (F_s) and freshwater transport (F_{ov}) at 34°S. The dots denote significance.

of increased isotherm depth at 34°S within a year (or longer) of strong Agulhas leakage transport. The signals cross the South Atlantic basin in around three years. The related wave speed is around $4\,cm/s$ which is in the range of both theoretical and observation-based wave speed estimates at these latitudes (Osychny and Cornillon, 2004; Webb et al., 2021). However, we cannot conclusively distinguish between Agulhas Rings, mesoscale eddies and Rossby waves since both would have the same
310 propagation speed.

   Another interesting aspect of the Agulhas leakage is not just the volume transport itself, but especially the amount of salt that is brought into the Atlantic Ocean. This salt transport is thought to be the main factor that is impacting the AMOC (Weijer and van Sebille, 2014) as most of the heat of the Agulhas leakage waters is lost to the atmosphere in the South Atlantic locally (Ivanciu et al., 2022). We find a mean northward freshwater transport of $0.1 \pm 0.03\,Sv$ over the simulation years 150-520
315 which remains positive during this entire time, indicating a stabilising salt-advection feedback. The correlation between the salt transport and the freshwater transport at 34°S (Figure 6) shows a strong negative correlation of -0.6 when F_S leads F_{ov} by three years, similar to the timescale between the Agulhas leakage and AMOC transports discussed above. This means that a stronger salt import from the Indian Ocean through Agulhas leakage reduces the freshwater transport. The salt input of the Agulhas leakage is mostly confined to the upper $1000\,m$, which relates to the depth of Agulhas rings (Schmid et al., 2003). We
320 note that the F_{ov} timeseries in the model has an increasing trend in the first 100 years and then decreases again. This impacts the detrending of the timeseries before calculating the correlations and leads to high correlations across all lead times. The peak at a 3-year lag remains robust even when increasing and decreasing parts of the time series are considered separately. In addition to the overturning component, the meridional freshwater transport in the Atlantic Ocean has an eddy component (Jüling et al., 2021). One could expect that the chaotic nature of Agulhas rings could lead to a connection here. However,
325 we do not find a significant correlation between the eddy component of the freshwater transport and the Agulhas leakage salt

transport. A caveat here is that the available timeseries necessary for the calculation was 150 years shorter than for the other data which influences the results, questioning its robustness.

4.5 The global overturning circulation under global warming

An important question is how the Agulhas leakage might change under climate change and what impacts this might have. Previous studies have suggested that an increase in Agulhas leakage due to changing wind patterns – an increase in magnitude and southward shift of the Southern Hemisphere westerlies (Cai, 2006) – over the region has been already happening during the past decades (Biastoch et al., 2009) and will continue into the future (Ivanciu et al., 2022). Here, we investigate this question using our three-member ensemble of historical and future transient simulations.
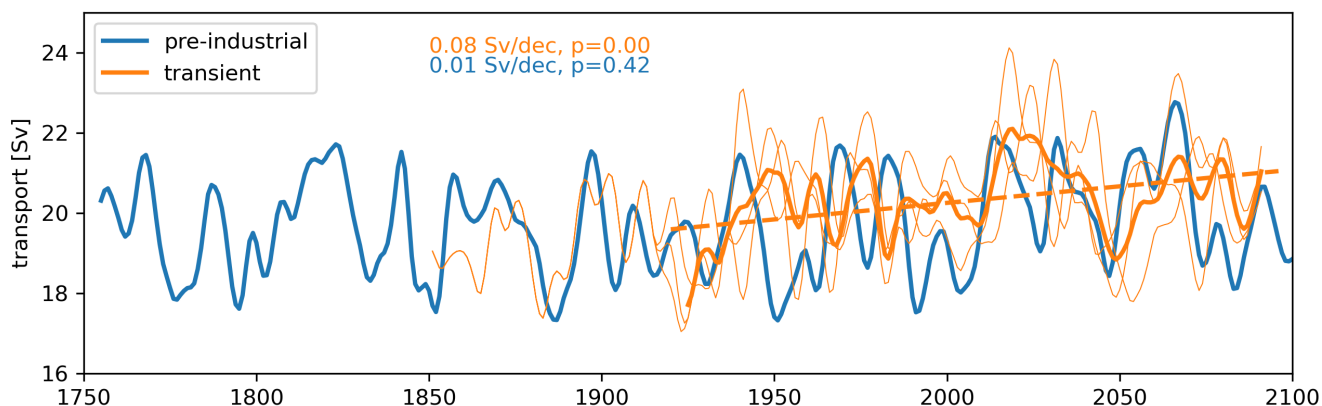
Figure 7. Decadally-filtered Agulhas leakage transport timeseries for PIcontrol, the ensemble mean of three members under historical and RCP8.5 forcing in the thick line, and individual members in the thin lines. Linear trend line and metrics for the period from 1920 to 2100 are also shown.

Figure 7 shows the timeseries of Agulhas leakage from the PIcontrol and of each ensemble member as well as their mean. We find an increase in Agulhas leakage of $0.08\,Sv/dec$ during the period from 1920 to 2100 in the ensemble mean. This trend is significant and also consistent between all three members with only negligibly different magnitudes. The PIcontrol shows a small, statistically insignificant trend of only $0.01\,Sv/dec$. The trend in the ensemble mean is lower by more than a factor of 2 from that reported in Ivanciu et al. (2022), i.e., about $0.2\,Sv/dec$. However, we note that the trend is sensitive to the period used in its calculation. For example, we do not find a discernible trend when calculating it for just the future forcing period, e.g., from 2005 to 2100. This finding is in contrast with changes in the Southern Hemisphere westerlies discussed above. To further investigate the changes in the winds, we calculate the Southern Annular Mode over that time period as a general representation of the wind field. The Southern Annular Mode in Figure 8 shows an increasing and stronger trend than the Agulhas leakage. However, an increase in the Southern Annular Mode can result from a variety of changes in the wind patterns, i.e., either a strengthening or a southward shift and also from regional distributions of these changes. Therefore, we take a closer look at

345   the wind metrics discussed earlier, considering the decadally-filtered ensemble-mean timeseries from historical and transient simulations (Figure A5). We find an increase in the maximum zonal windstress over the Indian Ocean as well as a southward shift of the latitude of the maximum zonal windstress, both statistically significant. This means that both changes impact the Southern Annular Mode similarly. Additionally, the wind stress curl increases significantly as well. These wind changes directly influence the dynamics of Agulhas leakage and lead to an increase in its transport. Why the resulting Agulhas leakage

350   response is lower than in Ivanciu et al. (2022) would need more systematic experiments and analyses, probably also with a larger ensemble number.
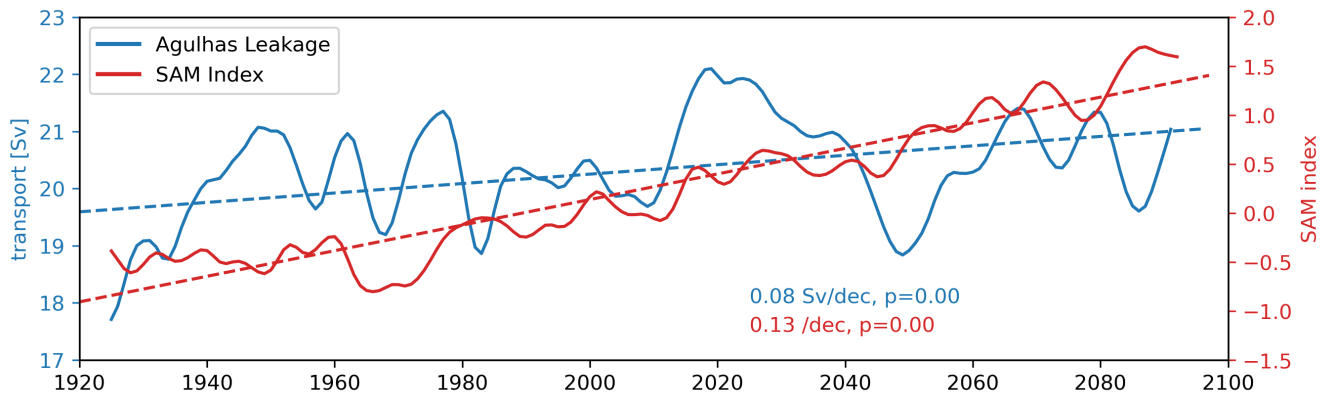
Figure 8. Agulhas leakage and Southern Annular Mode trends for the decadally-filtered ensemble average. Linear trend values and their significance for the period from 1920 to 2100 are also shown.

    Looking at the Agulhas Current, we find a strong negative trend under the greenhouse gas forcing, presented in Figure 9. The transport decreases by about $20\,Sv$ by 2100. There is a decrease in the trade winds over the Indian Ocean (Figure A2). Additionally, the wind stress curl over the southern sub-tropical gyre is decreasing as well. These lead to a decrease in the gyre

355   strength and its western boundary current, which comes out in the change of the Sverdrup transport at 32°S. This transport decreases by about $10\,Sv$ during the same time period. While these changes in the wind field can already account for 50% of the change in the Agulhas Current transport, another source in the Indian Ocean roughly contributes the other half: The transport through the ITF decreases by up to $8\,Sv$ until the end of the 21st century. These two changes add up to the total decrease in the Agulhas Current transport. The reduction in Agulhas Current transport ultimately leads to an increase in the Agulhas leakage

360   fraction. This means that a higher fraction of the Indian Ocean waters, even though reduced in absolute transport, end up in the Atlantic and that there is less recirculation.

    We finally investigate what role an increasing Agulhas leakage might have in the Atlantic Basin, specifically AMOC, in the future. Figure 10 shows timeseries of the ensemble means of Agulhas leakage, its salt transport, AMOC freshwater transport at 34°S and AMOC volume transport at 26°N. The increase in Agulhas leakage transport is also associated with a higher salt

365   transport into the Atlantic Ocean. We find that the salt transport via Agulhas leakage more than doubles from a pre-industrial mean of $0.24 \pm 0.25\,Sv\,psu$ to about $0.7\,Sv\,psu$ at the end of the 21st century and the trend specifically starts after 2000.
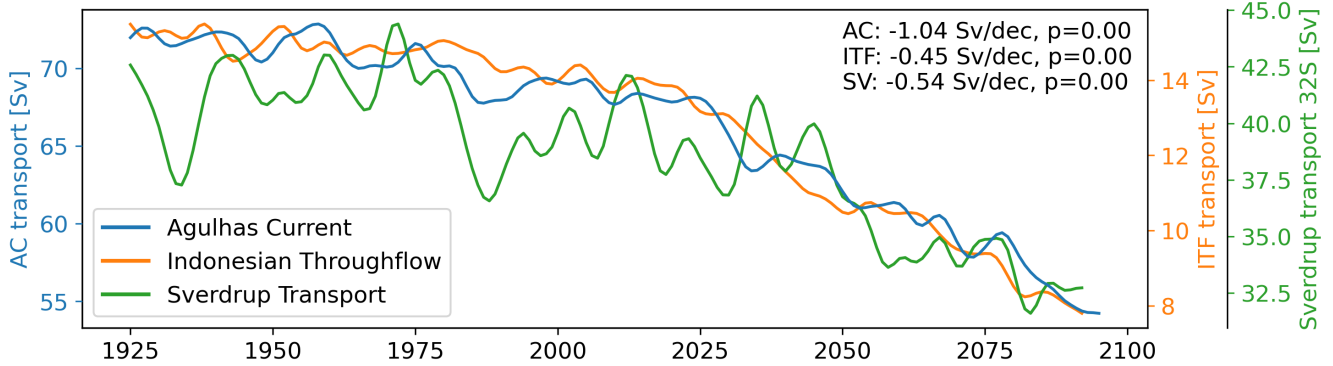
Figure 9. Decadally-filtered transport timeseries for the Agulhas Current, the Indonesian Throughflow (ITF), and the Sverdrup transport at 32°S. Dashed lines show the PIcontrol and the full thick lines the ensemble average under transient historical and RCP8.5 CO_2 forcing. The trend values are shown for the period from 1920 to 2100.

At a similar time, the freshwater transport at 34°S starts to decrease significantly down to $-0.05\,Sv$ by 2100, as does the AMOC transport down to about $11\,Sv$. While the AMOC decrease is most likely driven by processes in the North Atlantic (Weijer et al., 2019), the relation of the salt transport to the freshwater transport holds and it enhances the negative trend of the freshwater transport. This qualitatively describes a possible influence of the Agulhas leakage on AMOC that seems to increase in a warming climate.
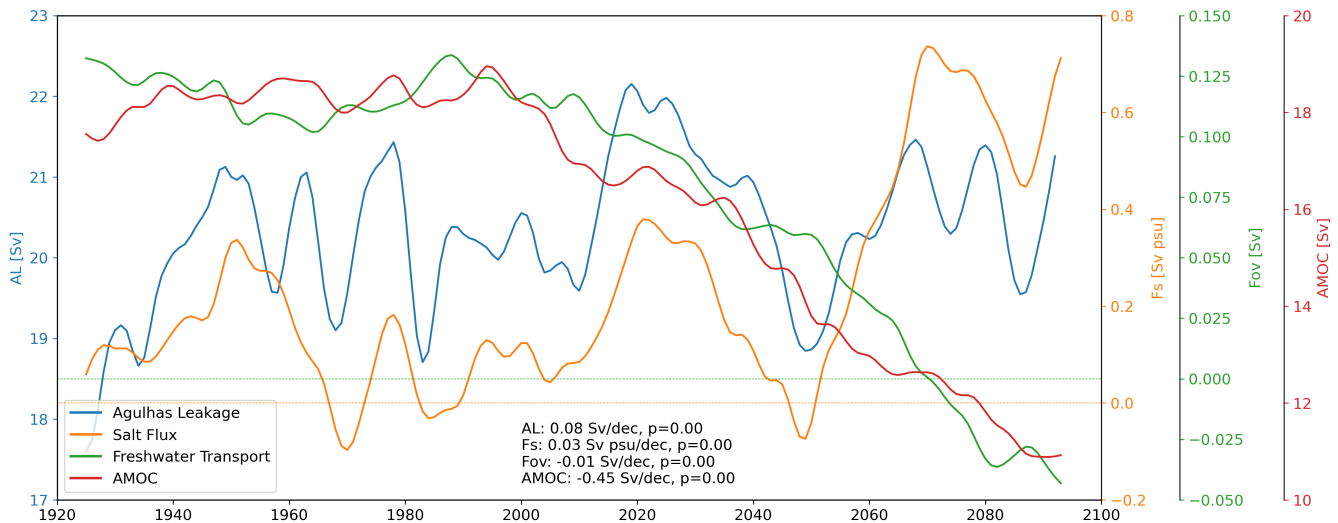
Figure 10. Decadally-filtered, ensemble-average timeseries of Agulhas leakage, Agulhas leakage salt transport (F_s) and AMOC freshwater transport (F_{ov}) at 34°S and AMOC volume transport at 26°N. Linear trend values and their significance for the period from 1920 to 2100 are also shown.

5 Discussion

The interoceanic transport of relatively warm and saline waters by Agulhas leakage is an important component of the large-scale ocean circulation and therefore global climate. Investigating how Agulhas leakage varies on longer timescales is thus essential to understand its impacts on the Atlantic Ocean in the presence of global warming.

Studies so far about the Agulhas leakage and its variability on long time scales were limited either by the short integration lengths of high-resolution model simulations or by the use of approximations to estimate the Agulhas leakage transport in models that do not properly represent the necessary dynamics due to their coarse resolutions. Here, we use a set of high-resolution and fully-coupled Earth system model simulations with the Community Earth System Model, CESM, with a 0.1° ocean (Chang et al., 2020). These simulations are a multi-centennial pre-industrial control run and a three-member ensemble of historical and transient CO_2-forcing experiments under an RCP8.5 scenario, the latter for after 2006. A brief evaluation of Dynamic Sea Level variability against satellite altimetry shows that the model captures the necessary scales in the Agulhas System as well as globally (Chang et al., 2020). The high resolution allows us to apply a Lagrangian particle tracking algorithm to calculate the Agulhas leakage transport precisely as the amount of water, that comes from the Agulhas Current and then flows into the Atlantic Ocean through the Good Hope section. Using these model simulations, we investigate the internal variability of Agulhas leakage on long timescales, its driving mechanisms, and impacts on the AMOC. Additionally, we examine how these relationships might evolve in the future under a warming climate.

Our analysis shows strong interannual variability, which is connected to the formation and propagation of Agulhas rings (Holton et al., 2017). On longer timescales, we find a significant spectral peak at a period of 14 years and strong but not significant peaks at 40-50 years. These peaks are not robust due to the rather high variability in this region, showing sensitivity to analysis methods and length of the timeseries. It can, of course, be the case that there is no robust internal variability of the system on these timescales. Nevertheless, further research is needed with longer high-resolution simulations.

Our results also show that the Agulhas leakage is driven by the overlying wind field, in agreement with previous work (Durgadoo et al., 2013), even though the direct mechanism is not quite clear yet (Rühs et al., 2022). Stronger westerlies winds are associated with a larger wind stress curl over the southern Indian Ocean which leads to an increase of the Agulhas leakage with a time lag of three to four years related to the time scales of baroclinic adjustment in the Indian Ocean. This process is similar to that of DiNezio et al. (2009), who relate transport changes in the Florida Current on interannual to decadal timescales to a change in the windstress curl to the east of that region. Nevertheless, the region where the winds are important determines the timescale of adjustment processes which could therefore vary between eastern or western parts of a relevant domain. We find the strongest correlation between Agulhas leakage and the windfield at 50°S and between 40°E and 60°E (Figure A3): A increase in the winds here leads to an increase in Agulhas leakage. A coherence analysis between the winds and the Agulhas leakage shows that the winds are the dominant driver of the system across timescales from years to decades.

Our analysis also identifies a significant positive correlation at zero lag for Agulhas leakage and the Agulhas Current strength. The zero year lag relates to the fact that we define the Agulhas leakage transport based on the release year of the particles within the Agulhas Current. Therefore, in our simulations, a stronger Agulhas Current leads to a stronger leakage, which

is in contrast to the results from Van Sebille et al. (2009), who found a negative correlation, while Loveday et al. (2014) described an insensitivity of the Agulhas leakage to the Agulhas Current's strength. The same analysis but for the AMOC strength at 34°S reveals a significant positive correlation when Agulhas leakage leads AMOC by 2 years. This time lag is not consistent with an advective transport timescale because the majority of the particles cross the domain within the first year. Further analysis suggests that the lag could be controlled by Rossby wave dynamics. We find westward propagating wave signals in the 10°C isotherm depth, which can be used as an indicator of Rossby waves (Olson and Evans, 1986). These waves take about 2-3 years to cross the South Atlantic Ocean, altering the geostrophic balance and consequently the AMOC transport. This wave connection has been suggested by Biastoch et al. (2008) as well to explain the time scales of interaction between Agulhas leakage and AMOC. Upon reaching the western boundary, the signal has the potential to be rapidly transported northward through topographic shelf waves and could thereby influence the AMOC further north. Sanchez-Franks et al. (2021) found Rossby waves to impact the AMOC in the North Atlantic along the RAPID array. However, it is not clear to distinguish between Rossby waves, mesoscale eddies and Agulhas Rings which propagate at similar speeds. Overall, the temporal variability of the AMOC cannot be solely linked to Agulhas leakage but is rather a combination of a series of different contributing factors including atmospheric forcing and other far-field influences. Further analysis are needed here to understand the exact connecting mechanism between Agulhas leakage and AMOC.

For the global overturning, the heat and salt transports are as important as the volume transport. By tracking the salinity along the particle track, we can evaluate the salt transport of the Agulhas leakage into the Atlantic. We then investigate the relationship of the salt transport to the freshwater transport induced by the overturning circulation at 34°S, which is part of the salt-advection feedback. This feedback describes a connection between the AMOC strength, the freshwater transport at 34°S, and the density difference between the North and the South Atlantic. The freshwater transport is positive in the pre-industrial control run, indicating a stable AMOC. The real ocean is thought to be in a bi-stable AMOC regime, hence a negative freshwater transport (Rahmstorf, 1996; Arumí-Planas et al., 2024). We note that there are configurations with other modelling frameworks that have a bi-stable AMOC, and Deshayes et al. (2013) show that stability also relates to model resolution with higher resolution leading to a negative freshwater transport. However, to complicate matters further, such AMOC stability varies between forced ocean-only experiments and fully-coupled Earth system models as well (Cheng et al., 2018). Van Westen and Dijkstra (2024) show that many coupled models have errors in their surface salinities due to atmospheric precipitation biases which then influences the freshwater transport in the ocean. They also show that models from the Climate Model Intercomparison Project phase 6 (CMIP6) have both positive and negative freshwater transports, but the ones with a negative transport underestimate the AMOC transport; no model gets both in the observational range. In this study we were able to identify a strong negative correlation between the salt transport and the freshwater transport across 34°S. Even though it is likely that changes in Agulhas leakage will have an impact on the stability of the AMOC, the strong trend of F_{ov}, including a sign change (Figure 10), does not allow a direct conclusion. Dedicated studies are required, optimally with sensitivity experiments using coupled models (e.g., Schulzki et al., 2024).

The 3-member ensemble of transient simulations under historical and RCP8.5 forcing shows an increase in the Agulhas leakage transport in response to the anthropogenic global warming, inline with previous study that also found stronger Agulhas

leakage transport under a warmer climate. The increase we find is not as strong as some other studies show or suggest (Ivanciu et al., 2022; Beech et al., 2022), but still significant. The reason for the modest increase in Agulhas leakage transport in our simulations lies in competing effects from the global circulation. On one hand, the wind field favours an enhanced Agulhas leakage transport through strengthened and southward shifted westerlies, as indicated by the strengthening in Southern Annular Mode. On the other hand, the projected weakening of the Agulhas Current transport, is conducive of weakening of the Agulhas leakage transport, by reason of the positive correlation between Agulhas leakage and the Agulhas Current previously identified in our analysis. The Agulhas Current is further impacted by Indian Ocean sources, both originating within and also brought in from the Pacific Ocean by the ITF (Durgadoo et al., 2017). Our results show that two factors almost equally contribute to the decline in the Agulhas Current: A reduction of the trade winds in the Indian Ocean contributing to a weaker western boundary current and a weaker ITF associated with reduced inflow of relatively warm and fresh water from Pacific Ocean origin into the Indian Ocean. The reduction of the ITF, and in consequence of the Agulhas Current transport, can be seen as a weakening of the global overturning, probably related to thermohaline causes. In another study, Hu et al. (2021) performed hosing experiments to force an AMOC collapse, which then leads to a reduction of $15\,Sv$ in the Agulhas Current and $10\,Sv$ in the Indonesian Throughflow in the first 100 years after the freshwater release, therefore similar magnitudes as we found. This further underlines that the whole Agulhas system is controlled by the global overturning circulation as well as local wind-driven dynamics.

Regarding the future evolution of the AMOC, we also see an increase in the salt transport of the Agulhas leakage. We calculate the salt transport as the difference of the particle salinities to the mean salinity at the crossing section. Van Westen and Dijkstra (2024) investigated the similar model runs, but at lower horizontal resolution, and found a change in the local salinity at the section during global warming due to more evaporation than precipitation, which then impacts the reference salinity for the salt transport estimation. However, when fitting a linear trend to the section and using this as a reference instead of just a mean, we do find a significant increase of the salt transport as well but with a smaller magnitude. As the salt transport trend is the strongest after 2000, opposite to the Agulhas leakage trend, it seems that this is based on a change in the hydrography rather than the volume transport. The increased salt transport then contributes to a decrease of the freshwater transport. Van Westen and Dijkstra (2024) also show that the decrease in the freshwater transport is salinity based and mostly depends on changes in the upper 1500m, which is consistent with the impact of the Agulhas leakage salt transport. However, the freshwater transport as a metric for AMOC stability only really holds under equilibrium conditions (Rahmstorf, 1996). Additionally, the change of the AMOC due to global warming also strongly depends on the initial AMOC state (Liu et al., 2017). As our simulations do not reach an equilibrium by 2100, the discussion on a potential connection between Agulhas leakage and the stability of the AMOC has to be considered with care and would require a set of sensitivity experiments that is beyond this study. The hypothesis remains that the salt input from the Agulhas leakage into the Atlantic ultimately reaches the North Atlantic and deep water formation regions (Weijer and van Sebille, 2014). The salt can then play a role in setting the local stratification and thereby positively impacting deep water formation north of south the Greenland-Scotland Ridge. This has been described in coupled model experiments by Schulzki et al. (2024). However, owing to the long timescales involved, the direct quantification of these processes and the question on the stability of the AMOC strength needs further research. For this

purpose, one would need ensemble experiments with eddy-rich Atlantic-wide or global configurations and long experiments with predicted or idealised freshwater hosing.

6   Conclusions

A set of unprecedentedly long high-resolution CESM simulations allowed us to perform an extended analysis of the Agulhas Current system and the interoceanic transports associated with Agulhas leakage. In the pre-industrial climate, our analysis shows that Agulhas leakage variability is driven by variation in the wind field over the southern Indian Ocean, in agreement with earlier findings. Furthermore, we show that Agulhas leakage is related to the strength of the Agulhas Current, with a stronger current leading to enhanced Agulhas leakage transport. Agulhas leakage is found to impact the AMOC through Rossby wave dynamics and/or mesoscale eddies and Agulhas Rings that propagate into the Atlantic Ocean. The salt transport of Agulhas leakage into the Atlantic influences the meridional freshwater transport induced by the AMOC and consequently AMOC stability through the salt-advection feedback. Agulhas leakage is projected to increase under global warming due to strengthening of the westerly winds in the Southern Hemisphere in the CESM 3-member ensemble of high-resolution transient simulations. However, the projected Agulhas leakage increase in our simulations is weaker than previously reported. This weaker increase in Agulhas leakage is imputable to the combination of a strong reduction of the Agulhas Current transport which is the result of both a decreased wind-related Sverdrup transport, and a reduction of the Indonesian Throughflow. Nevertheless, the moderate Agulhas leakage increase under a warming climate is accompanied by an increasing salt transport that could play a role in the stability of the AMOC. This study sketches a new picture of the role of Agulhas leakage in the climate system through a fully coupled eddy-rich earth system model. It also highlights points that will need further research attention, such as the exact connecting mechanism between Agulhas leakage and AMOC and the relevance of the increased salt input into the Atlantic Ocean on AMOC stability in comparison to other factors in play.

Code and data availability. The data and material that support the findings of this study are available through GEOMAR at https://hdl.handle.net/20.500.12085/f10e76e5-0e1e-4dee-95b5-45d6275eb144 (Grosselindemann et al., 2024).

Author contributions. AB and GD initiated and designed the analysis. HG led the paper and wrote and structured the manuscript. HG performed all the analyses under supervision from all authors. All authors discussed the analyses and provided comments to the text.

Competing interests. The authors declare no competing interests.

Acknowledgements. The high-resolution CESM simulations were initiated by the International Laboratory for High-Resolution Earth System Prediction – a collaboration between the Qingdao Pilot National Laboratory for Marine Science and Technology, Texas A&M University, and the US National Science Foundation (NSF) National Center for Atmospheric Research (NCAR). A major portion of the high-resolution CESM simulations were completed on Frontera at the Texas Advanced Computing Center (TACC) of the University of Texas at Austin, TX, US, under project number ATM20005. F.C. was partly supported by the NSF grant AGS-2231237. This material is based upon work supported by the NSF NCAR, which is a major facility sponsored by the NSF under Cooperative Agreement 1852977. HG was supported by a scholarship of the Prof. Dr. Werner Petersen Stiftung and a DAAD PROMOS fellowship from the Christian-Albrechts University in Kiel.

505
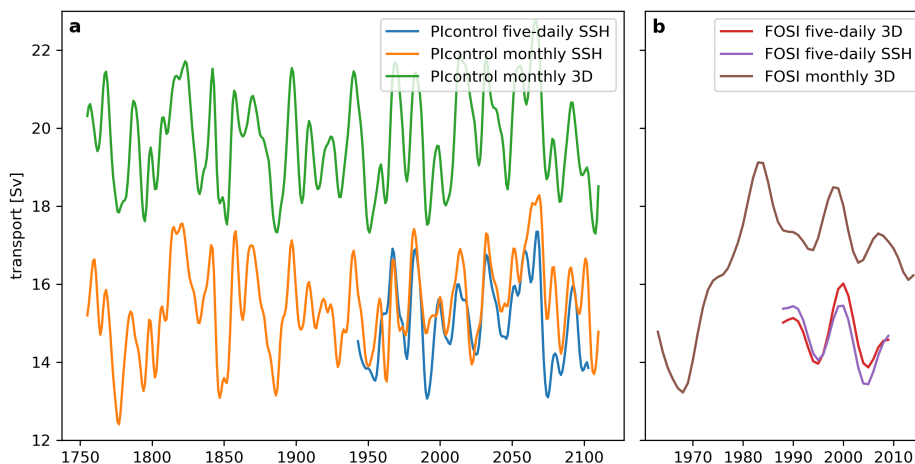
Figure A1. Decadally-filtered transport timeseries of Agulhas leakage from all approaches; CESM1.3 fully-coupled PIcontrol in (a), forced ocean sea-ice (FOSI) in (b). See Section 3.1 for details.
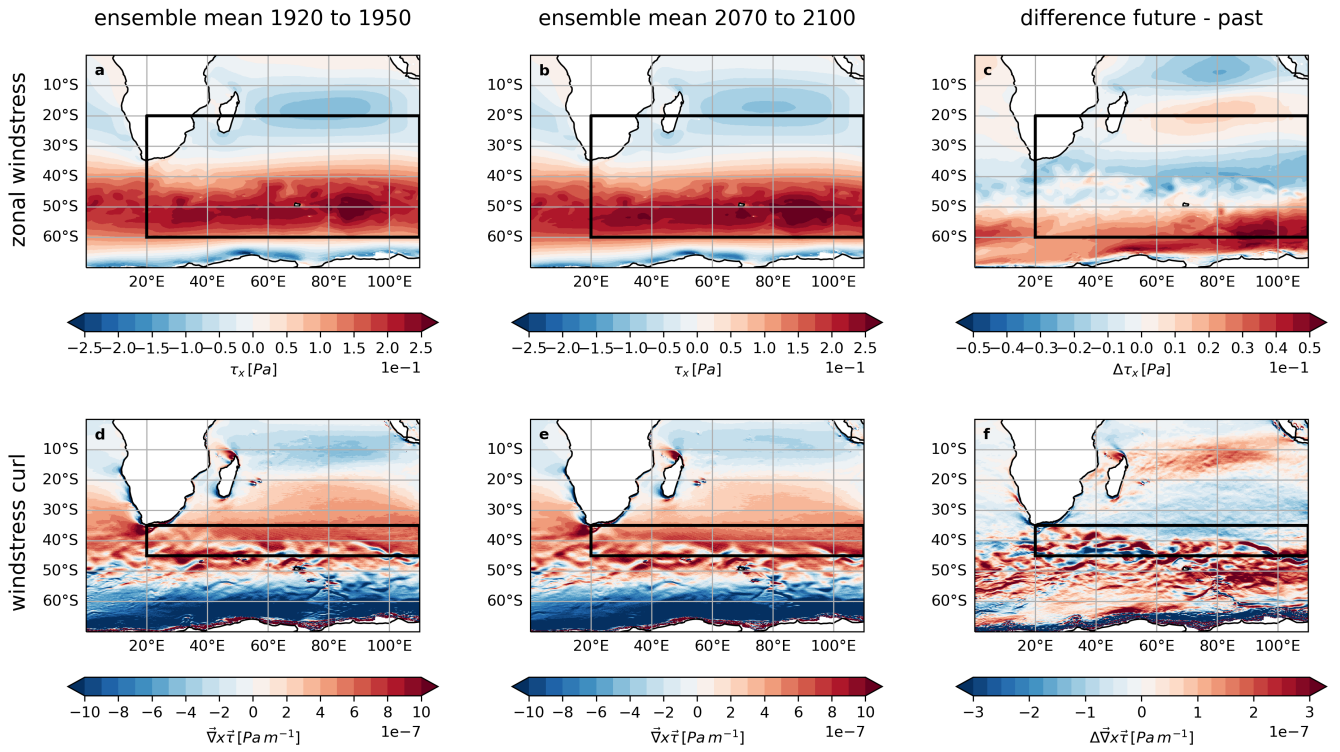
Figure A2. Ensemble-averaged zonal windstress τ_x (a-c) and windstress curl $\nabla \times \tau$ (d-f) historical (a,d) and future (b,e) mean states for the periods from 1920 to 1950 and 2070 to 2100, respectively, and their change (c,f), the periods were chosen to represent a mean climate state at the begin and end of the simulation period, boxes show areas used to calculate wind metrics for Figure 5 and Figure A5
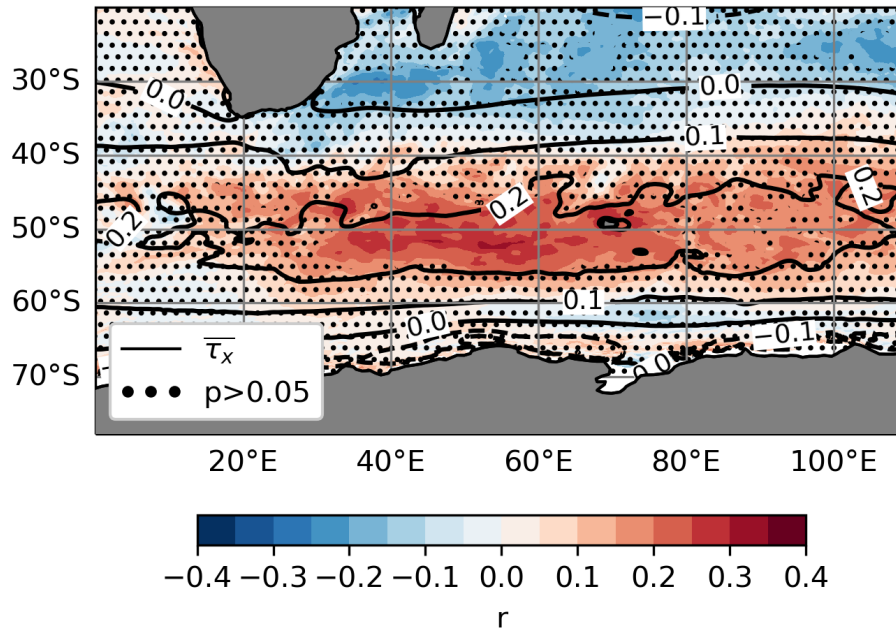
Figure A3. Correlation of Agulhas leakage transport with the annual-mean zonal windstress at each grid point for PIcontrol. Correlations are not significant in the dotted regions. Contour lines show the mean zonal windstress in N m^{-2}.
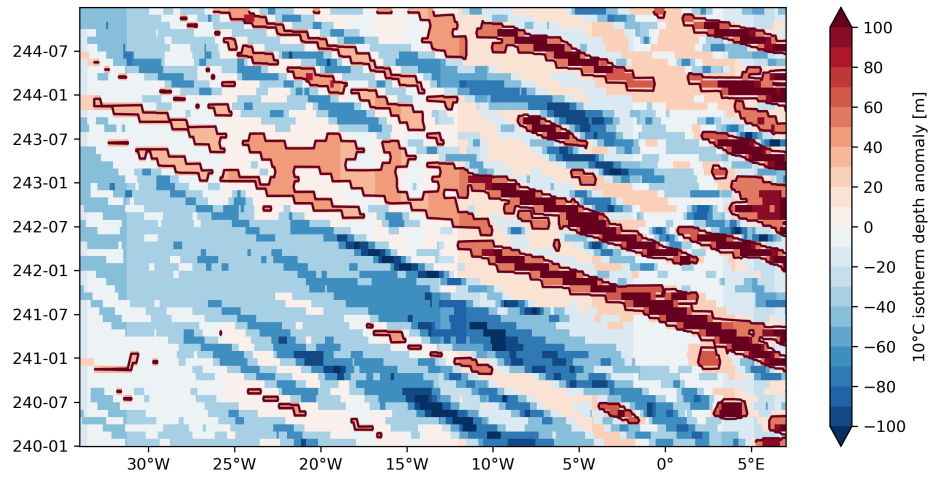
Figure A4. Timeseries of the 10°C isotherm depth anomaly from PIcontrol for years 240 to 245 as a function of longitude and at 34°S. The 30-m depth is shown as a contour line.
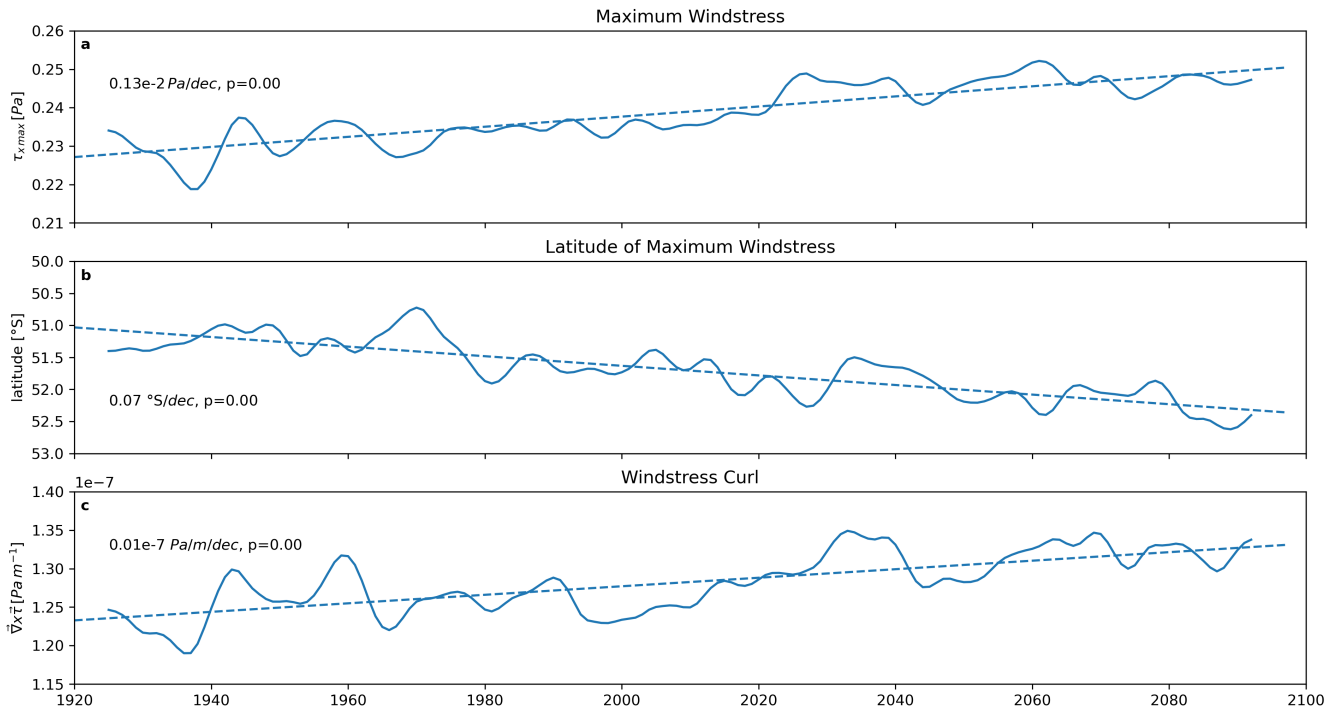
Figure A5. Timeseries and trends for the period from 1920 to 2100 maximum zonal wind stress $\tau_{x\,max}$ (a), latitude of the maximum zonal windstress in °S (b), and average wind stress curl $\nabla \times \tau$ (c) as decadally-filtered ensemble means, trends are calculated on unfiltered data.

References

Anderson, D. L. and Killworth, P. D.: Spin-up of a stratified ocean, with topography, Deep-Sea Research, 24, 709–732, https://doi.org/10.1016/0146-6291(77)90495-7, 1977.

Arumí-Planas, C., Dong, S., Perez, R., Harrison, M. J., Farneti, R., and Hernández-Guerra, A.: A Multi-Data Set Analysis of the Freshwater Transport by the Atlantic Meridional Overturning Circulation at Nominally 34.5°S, Journal of Geophysical Research: Oceans, 129, https://doi.org/10.1029/2023JC020558, 2024.

Bars, D. L., Dijkstra, H. A., and Ruijter, W. P. M. D.: Impact of the Indonesian Throughflow on Agulhas leakage, Ocean Science, 9, 773–785, https://doi.org/10.5194/os-9-773-2013, 2013.

Beal, L. M., Ruijter, W. P. D., Biastoch, A., Zahn, R., Cronin, M., Hermes, J., Lutjeharms, J., Quartly, G., Tozuka, T., Baker-Yeboah, S., Bornman, T., Cipollini, P., Dijkstra, H., Hall, I., Park, W., Peeters, F., Penven, P., Ridderinkhof, H., and Zinke, J.: On the role of the Agulhas system in ocean circulation and climate, Nature, 472, 429–436, https://doi.org/10.1038/nature09983, 2011.

Beal, L. M., Elipot, S., Houk, A., and Leber, G. M.: Capturing the transport variability of a western boundary jet: Results from the Agulhas Current time-series experiment (ACT), Journal of Physical Oceanography, 45, 1302–1324, https://doi.org/10.1175/JPO-D-14-0119.1, 2015.

Beech, N., Rackow, T., Semmler, T., Danilov, S., Wang, Q., and Jung, T.: Long-term evolution of ocean eddy activity in a warming world, Nature Climate Change, 12, 910–917, https://doi.org/10.1038/s41558-022-01478-3, 2022.

Biastoch, A., Böning, C. W., and Lutjeharms, J. R.: Agulhas leakage dynamics affects decadal variability in Atlantic overturning circulation, Nature, 456, 489–492, https://doi.org/10.1038/nature07426, 2008.

Biastoch, A., Böning, C. W., Schwarzkopf, F. U., and Lutjeharms, J. R.: Increase in Agulhas leakage due to poleward shift of Southern Hemisphere westerlies, Nature, 462, 495–498, https://doi.org/10.1038/nature08519, 2009.

Biastoch, A., Durgadoo, J. V., Morrison, A. K., Van Sebille, E., Weijer, W., and Griffies, S. M.: Atlantic multi-decadal oscillation covaries with Agulhas leakage, Nature Communications, 6, https://doi.org/10.1038/ncomms10082, 2015.

Boers, N.: Observation-based early-warning signals for a collapse of the Atlantic Meridional Overturning Circulation, Nature Climate Change, 11, 680–688, https://doi.org/10.1038/s41558-021-01097-4, 2021.

Boulton, C. A., Allison, L. C., and Lenton, T. M.: Early warning signals of atlantic meridional overturning circulation collapse in a fully coupled climate model, Nature Communications, 5, https://doi.org/10.1038/ncomms6752, 2014.

Cai, W.: Antarctic ozone depletion causes an intensification of the Southern Ocean super-gyre circulation, Geophysical Research Letters, 33, 1–4, https://doi.org/10.1029/2005GL024911, 2006.

Chang, P., Zhang, S., Danabasoglu, G., Yeager, S. G., Fu, H., Wang, H., Castruccio, F. S., Chen, Y., Edwards, J., Fu, D., Jia, Y., Laurindo, L. C., Liu, X., Rosenbloom, N., Small, R. J., Xu, G., Zeng, Y., Zhang, Q., Bacmeister, J., Bailey, D. A., Duan, X., DuVivier, A. K., Li, D., Li, Y., Neale, R., Stössel, A., Wang, L., Zhuang, Y., Baker, A., Bates, S., Dennis, J., Diao, X., Gan, B., Gopal, A., Jia, D., Jing, Z., Ma, X., Saravanan, R., Strand, W. G., Tao, J., Yang, H., Wang, X., Wei, Z., and Wu, L.: An unprecedented set of high-resolution earth system simulations for understanding multiscale interactions in climate variability and change, Journal of Advances in Modeling Earth Systems, 12, https://doi.org/10.1029/2020MS002298, 2020.

Cheng, W., Weijer, W., Kim, W. M., Danabasoglu, G., Yeager, S. G., Gent, P. R., Zhang, D., Chiang, J. C., and Zhang, J.: Can the salt-advection feedback be detected in internal variability of the atlantic meridional overturning circulation?, Journal of Climate, 31, 6649–6667, https://doi.org/10.1175/JCLI-D-17-0825.1, 2018.

545 Cheng, Y., Putrasahan, D., Beal, L., and Kirtman, B.: Quantifying Agulhas Leakage in a high-resolution climate model, Journal of Climate, 29, 6881–6892, https://doi.org/10.1175/JCLI-D-15-0568.1, 2016.

CMEMS: Atlantic Meridional Overturning Circulation AMOC timeseries at 26N from Reanalysis, https://doi.org/https://doi.org/10.48670/moi-00232, 2023.

Daher, H., Beal, L. M., and Schwarzkopf, F. U.: A new improved estimation of Agulhas Leakage using observations and simulations of
550 Lagrangian floats and drifters, Journal of Geophysical Research: Oceans, 125, 1–17, https://doi.org/10.1029/2019JC015753, 2020.

Danabasoglu, G., Bates, S. C., Briegleb, B. P., Jayne, S. R., Jochum, M., Large, W. G., Peacock, S., and Yeager, S. G.: The CCSM4 ocean component, Journal of Climate, 25, 1361–1389, https://doi.org/10.1175/JCLI-D-11-00091.1, 2012.

Delandmeter, P. and Van Sebille, E.: The Parcels v2.0 Lagrangian framework: New field interpolation schemes, Geoscientific Model Development, 12, 3571–3584, https://doi.org/10.5194/gmd-12-3571-2019, 2019.

555 Dencausse, G., Arhan, M., and Speich, S.: Routes of Agulhas rings in the southeastern Cape Basin, Deep-Sea Research Part I: Oceanographic Research Papers, 57, 1406–1421, https://doi.org/10.1016/j.dsr.2010.07.008, 2010.

Deshayes, J., Tréguier, A.-M., Barnier, B., Lecointre, A., Sommer, J. L., Molines, J.-M., Penduff, T., Bourdallé-Badie, R., Drillet, Y., Garric, G., Benshila, R., Madec, G., Biastoch, A., Böning, C. W., Scheinert, M., Coward, A. C., and Hirschi, J. J.: Oceanic hindcast simulations at high resolution suggest that the Atlantic MOC is bistable, Geophysical Research Letters, 40, 3069–3073,
560 https://doi.org/10.1002/grl.50534, 2013.

DiNezio, P. N., Gramer, L. J., Johns, W. E., Meinen, C. S., and Baringer, M. O.: Observed interannual variability of the Florida current: Wind forcing and the North Atlantic Oscillation, Journal of Physical Oceanography, 39, 721–736, https://doi.org/10.1175/2008JPO4001.1, 2009.

Durgadoo, J. V., Loveday, B. R., Reason, C. J. C., Penven, P., and Biastoch, A.: Agulhas Leakage predominantly responds to the southern hemisphere westerlies, Journal of Physical Oceanography, 43, 2113–2131, https://doi.org/10.1175/JPO-D-13-047.1, 2013.

565 Durgadoo, J. V., Rühs, S., Biastoch, A., and Böning, C. W. B.: Indian Ocean sources of Agulhas leakage, Journal of Geophysical Research: Oceans, 122, 3481–3499, https://doi.org/10.1002/2016JC012676, 2017.

Gordon, A. L.: Interocean exchange of thermocline water, Journal of Geophysical Research, 91, 5037, https://doi.org/10.1029/JC091iC04p05037, 1986.

Gordon, A. L., Bosley, K. T., and Aikman, F.: Tropical atlantic water within the Benguela upwelling system at 27°S, Deep-Sea Research Part
570 I, 42, 1–12, https://doi.org/10.1016/0967-0637(94)00032-N, 1995.

Grosselindemann, H., Castruccio, F., Danabasoglu, G., and Biastoch, A.: Supplementary data to Grosselindemann et al. (2024): Long-term Variability and Trends of Agulhas Leakage and its Impacts on the Global Overturning, https://hdl.handle.net/20.500.12085/f10e76e5-0e1e-4dee-95b5-45d6275eb144, 2024.

Holton, L., Deshayes, J., Backeberg, B. C., Loveday, B. R., Hermes, J. C., and Reason, C. J. C.: Spatio-temporal characteristics of Agulhas
575 leakage: a model inter-comparison study, Climate Dynamics, 48, 2107–2121, https://doi.org/10.1007/s00382-016-3193-5, 2017.

Hu, A., Meehl, G. A., Rosenbloom, N., Molina, M. J., and Strand, W. G.: The influence of variability in meridional overturning on global ocean circulation, Journal of Climate, 34, 7697–7716, https://doi.org/10.1175/JCLI-D-21-0119.1, 2021.

Hunke, E. C. and Lipscomb, W. H.: CICE: the Los Alamos sea ice model user's manual, version 4., Los Alamos National Laboratory Tech. Rep, 2008.

580 Ivanciu, I., Matthes, K., Biastoch, A., Wahl, S., and Harlaß, J.: Twenty-first-century Southern Hemisphere impacts of ozone recovery and climate change from the stratosphere to the ocean, Weather and Climate Dynamics, 3, 139–171, https://doi.org/10.5194/wcd-3-139-2022, 2022.

Jüling, A., Zhang, X., Castellana, D., Heydt, A. S. V. D., and Dijkstra, H. A.: The atlantic's freshwater budget under climate change in the community earth system model with strongly eddying oceans, Ocean Science, 17, 729–754, https://doi.org/10.5194/os-17-729-2021, 2021.

Kehl, C., Nooteboom, P. D., Kaandorp, M. L., and van Sebille, E.: Efficiently simulating Lagrangian particles in large-scale ocean flows — Data structures and their impact on geophysical applications, Computers and Geosciences, 175, 105 322, https://doi.org/10.1016/j.cageo.2023.105322, 2023.

Lawrence, D. M., Oleson, K. W., Flanner, M. G., Thornton, P. E., Swenson, S. C., Lawrence, P. J., Zeng, X., Yang, Z.-L., Levis, S., Sakaguchi, K., Bonan, G. B., and Slater, A. G.: Parameterization improvements and functional and structural advances in Version 4 of the Community Land Model, Journal of Advances in Modeling Earth Systems, 3, 1–27, https://doi.org/10.1029/2011ms000045, 2011.

Li, J., Roughan, M., and Kerry, C.: Drivers of ocean warming in the western boundary currents of the Southern Hemisphere, Nature Climate Change, 12, 901–909, https://doi.org/10.1038/s41558-022-01473-8, 2022.

Liu, W., Xie, S.-P., Liu, Z., and Zhu, J.: Overlooked possibility of a collapsed Atlantic Meridional Overturning Circulation in warming climate, Science Advances, 3, https://doi.org/10.1126/sciadv.1601666, 2017.

Lohmann, J., Dijkstra, H. A., Jochum, M., Lucarini, V., and Ditlevsen, P. D.: Multistability and intermediate tipping of the Atlantic Ocean circulation, Science Advances, 10, 4253, https://doi.org/10.1126/sciadv.adi4253, 2024.

Loveday, B. R., Durgadoo, J. V., Reason, C. J., Biastoch, A., and Penven, P.: Decoupling of the Agulhas leakage from the Agulhas Current, Journal of Physical Oceanography, 44, 1776–1797, https://doi.org/10.1175/JPO-D-13-093.1, 2014.

Makarim, S., Sprintall, J., Liu, Z., Yu, W., Santoso, A., Yan, X. H., and Susanto, R. D.: Previously unidentified Indonesian Throughflow pathways and freshening in the Indian Ocean during recent decades, Scientific Reports, 9, 1–13, https://doi.org/10.1038/s41598-019-43841-z, 2019.

Meehl, G. A., Yang, D., Arblaster, J. M., Bates, S. C., Rosenbloom, N., Neale, R., Bacmeister, J., Lauritzen, P. H., Bryan, F., Small, J., Truesdale, J., Hannay, C., Shields, C., Strand, W. G., Dennis, J., and Danabasoglu, G.: Effects of model resolution, physics, and coupling on southern hemisphere storm tracks in CESM1.3, Geophysical Research Letters, 46, 12 408–12 416, https://doi.org/10.1029/2019GL084057, 2019.

Mertz, F., Rosmorduc, V., Maheu, C., and Faugere, Y.: For sea level SLA products, Copernicus Marine Service, 1, 1–51, 2017.

Moat, B., Smeed, D., Rayner, D., Johns, W., Smith, R., Volkov, D., Baringer, M., and Collins, J.: Atlantic meridional overturning circulation observed by the RAPID-MOCHA-WBTS (RAPID-Meridional Overturning Circulation and Heatflux Array-Western Boundary Time Series) array at 26N from 2004 to 2022 (v2022.1), https://doi.org/10.5285/04c79ece-3186-349a-e063-6c86abc0158c, 2023.

Morrow, R., Ward, M. L., Hogg, A. M., and Pasquet, S.: Eddy response to Southern Ocean climate modes, Journal of Geophysical Research: Oceans, 115, 1–12, https://doi.org/10.1029/2009JC005894, 2010.

Neale, R. B., Gettelman, A., Park, S., Chen, C.-C., Lauritzen, P. H., Williamson, D. L., Conley, A. J., Kinnison, D., Marsh, D., Smith, A. K., Vitt, F. M., Garcia, R., Lamarque, J.-F., Mills, M. J., Tilmes, S., Morrison, H., Cameron-Smith, P., D, W., and M, C.: Description of the NCAR Community Atmosphere Model (CAM5.0), 2012.

Olson, D. B. and Evans, R. H.: Rings of the Agulhas current, Deep Sea Research Part A, Oceanographic Research Papers, 33, 27–42, https://doi.org/10.1016/0198-0149(86)90106-8, 1986.

Osychny, V. and Cornillon, P.: Properties of Rossby waves in the North Atlantic estimated from satellite data, Journal of Physical Oceanography, 34, 61–76, https://doi.org/10.1175/1520-0485(2004)034<0061:PORWIT>2.0.CO;2, 2004.

620   Phillips, A. S., Deser, C., and Fasullo, J.: Evaluating modes of variability in climate models, Eos (United States), 95, 453–455, https://doi.org/10.1002/2014EO490002, 2014.

Rahmstorf, S.: On the freshwater forcing and transport of the Atlantic thermohaline circulation, Climate Dynamics, 12, 799–811, https://doi.org/10.1007/s003820050144, 1996.

Roberts, M. J., Jackson, L. C., Roberts, C. D., Meccia, V., Docquier, D., Koenigk, T., Ortega, P., Moreno-Chamarro, E., Bellucci, A., Coward,

625   A., Drijfhout, S., Exarchou, E., Gutjahr, O., Hewitt, H., Iovino, D., Lohmann, K., Putrasahan, D., Schiemann, R., Seddon, J., Terray, L., Xu, X., Zhang, Q., Chang, P., Yeager, S. G., Castruccio, F. S., Zhang, S., and Wu, L.: Sensitivity of the Atlantic Meridional Overturning Circulation to model resolution in CMIP6 HighResMIP simulations and implications for future changes, Journal of Advances in Modeling Earth Systems, 12, 1–22, https://doi.org/10.1029/2019MS002014, 2020.

Rühs, S., Schwarzkopf, F. U., Speich, S., and Biastoch, A.: Cold vs. warm water route-sources for the upper limb of the Atlantic Meridional

630   Overturning Circulation revisited in a high-resolution ocean model, Ocean Science, 15, 489–512, https://doi.org/10.5194/os-15-489-2019, 2019.

Rühs, S., Schmidt, C., Schubert, R., Schulzki, T. G., Schwarzkopf, F. U., Bars, D. L., and Biastoch, A.: Robust estimates for the decadal evolution of Agulhas leakage from the 1960s to the 2010s, Communications Earth and Environment, 3, 318, https://doi.org/10.1038/s43247-022-00643-y, 2022.

635   Sanchez-Franks, A., Frajka-Williams, E., Moat, B. I., and Smeed, D. A.: A dynamically based method for estimating the Atlantic meridional overturning circulation at 26°N from satellite altimetry, Ocean Science, 17, 1321–1340, https://doi.org/10.5194/os-17-1321-2021, 2021.

Schmid, C., Boebel, O., Zenk, W., Lutjeharms, J. R., Garzoli, S. L., Richardson, P. L., and Barron, C.: Early evolution of an Agulhas Ring, Deep-Sea Research Part II: Topical Studies in Oceanography, 50, 141–166, https://doi.org/10.1016/S0967-0645(02)00382-X, 2003.

Schmidt, C., Schwarzkopf, F. U., Rühs, S., and Biastoch, A.: Characteristics and robustness of Agulhas leakage estimates: An inter-

640   comparison study of Lagrangian methods, Ocean Science, 17, 1067–1080, https://doi.org/10.5194/os-17-1067-2021, 2021.

Schouten, M. W., Ruijter, W. P. D., Van Leeuwen, P. J., and Lutjeharms, J. R.: Translation, decay and splitting of Agulhas rings in the southeastern Atlantic Ocean, Journal of Geophysical Research: Oceans, 105, 21 913–21 925, https://doi.org/10.1029/1999jc000046, 2000.

Schubert, R., Gula, J., and Biastoch, A.: Submesoscale flows impact Agulhas leakage in ocean simulations, Communications Earth and Environment, 2, 1–8, https://doi.org/10.1038/s43247-021-00271-y, 2021.

645   Schulzki, T., Schwarzkopf, F. U., and Biastoch, A.: Atlantic meridional overturning response to increased Southern Ocean wind stress in a climate model with an eddy-rich ocean, Journal of Climate, https://doi.org/10.1175/jcli-d-23-0727.1, 2024.

Smith, R., Jones, P., Briegleb, B., Bryan, F., Danabasoglu, G., Dennis, J., Dukowicz, J., Eden, C., Fox-Kemper, B., Gent, P., et al.: The parallel ocean program (POP) reference manual ocean component of the community climate system model (CCSM) and community earth system model (CESM), LAUR-01853, 141, 1–140, 2010.

650   Speich, S., Blanke, B., and Cai, W.: Atlantic meridional overturning circulation and the Southern Hemisphere supergyre, Geophysical Research Letters, 34, 1–5, https://doi.org/https://doi.org/10.1029/2007GL031583, 2007.

Speich, S., Rusciano, E., and Faure, V.: GOODHOPE/SAMOC, World, 29, 3, https://www.coriolis.eu.org/Science2/Atlantic-Ocean/GOODHOPE-SAMOC, 2023.

Stommel, H.: Thermohaline convection with two stable regimes of flow, Tellus, 13, 224–230, https://doi.org/10.3402/tellusa.v13i2.9491,

655   1961.

Sverdrup, H. U.: Wind-driven currents in a baroclinic ocean; with application to the equatorial currents of the eastern Pacific, Proceedings of the National Academy of Sciences, 33, 318–326, https://doi.org/10.1073/pnas.33.11.318, 1947.

Thompson, D. W. J. and Wallace, J. M.: Annular modes in the extratropical circulation. Part I: Month-to-month variability, Journal of Climate, 13, 1000–1016, https://doi.org/https://doi.org/10.1175/1520-0442(2000)013<1000:AMITEC>2.0.CO;2, 2000.

660 Thompson, R. O. R. Y.: Coherence Significance Levels, Journal of the Atmospheric Sciences, 36, 2020–2021, https://doi.org/10.1175/1520-0469(1979)036<2020:CSL>2.0.CO;2, 1979.

Torrence, C. and Compo, G. P.: A practical guide to wavelet analysis, Bulletin of the American Meteorological Society, 79, 61–78, https://doi.org/10.1175/1520-0477(1998)079<0061:APGTWA>2.0.CO;2, 1998.

Tsujino, H., Urakawa, S., Nakano, H., Small, R. J., Kim, W. M., Yeager, S. G., Danabasoglu, G., Suzuki, T., Bamber, J. L., Bentsen, M.,

665 Böning, C. W., Bozec, A., Chassignet, E. P., Curchitser, E., Dias, F. B., Durack, P. J., Griffies, S. M., Harada, Y., Ilicak, M., Josey, S. A., Kobayashi, C., Kobayashi, S., Komuro, Y., Large, W. G., Sommer, J. L., Marsland, S. J., Masina, S., Scheinert, M., Tomita, H., Valdivieso, M., and Yamazaki, D.: JRA-55 based surface dataset for driving ocean–sea-ice models (JRA55-do), Ocean Modelling, 130, 79–139, https://doi.org/10.1016/j.ocemod.2018.07.002, 2018.

Van Sebille, E., Biastoch, A., Van Leeuwen, P. J., and Ruijter, W. P. D.: A weaker Agulhas current leads to more Agulhas leakage, Geophysical

670 Research Letters, 36, 10–13, https://doi.org/10.1029/2008GL036614, 2009.

Van Sebille, E., Griffies, S. M., Abernathey, R., Adams, T. P., Berloff, P., Biastoch, A., Blanke, B., Chassignet, E. P., Cheng, Y., Cotter, C. J., Deleersnijder, E., Döös, K., Drake, H. F., Drijfhout, S., Gary, S. F., Heemink, A. W., Kjellsson, J., Koszalka, I. M., Lange, M., Lique, C., MacGilchrist, G. A., Marsh, R., Adame, C. G. M., McAdam, R., Nencioli, F., Paris, C. B., Piggott, M. D., Polton, J. A., Rühs, S., Shah, S. H., Thomas, M. D., Wang, J., Wolfram, P. J., Zanna, L., and Zika, J. D.: Lagrangian ocean analysis: Fundamentals and practices, Ocean

675 Modelling, 121, 49–75, https://doi.org/10.1016/j.ocemod.2017.11.008, 2018.

Van Vuuren, D. P., Edmonds, J., Kainuma, M., Riahi, K., Nakicenovic, N., Smith, S. J., and Rose, S. K.: The representative concentration pathways : an overview, Climatic Change, pp. 5–31, https://doi.org/10.1007/s10584-011-0148-z, 2011.

Van Westen, R. M. and Dijkstra, H. A.: Persistent climate model biases in the Atlantic Ocean's freshwater transport, Ocean Science, 20, 549–567, https://doi.org/10.5194/os-20-549-2024, 2024.

680 Van Westen, R. M., Kliphuis, M., and Dijkstra, H. A.: Physics-based early warning signal shows that AMOC is on tipping course, Science Advances, 10, https://doi.org/10.1126/sciadv.adk1189, 2024.

Webb, D. J., Spence, P., Holmes, R. M., and England, M. H.: Planetary-wave-induced strengthening of the AMOC forced by poleward intensified southern hemisphere westerly winds, Journal of Climate, 34, 7073–7090, https://doi.org/10.1175/JCLI-D-20-0858.1, 2021.

Weijer, W. and van Sebille, E.: Impact of Agulhas leakage on the Atlantic overturning circulation in the CCSM4, Journal of Climate, 27,

685 101–110, https://doi.org/10.1175/JCLI-D-12-00714.1, 2014.

Weijer, W., Cheng, W., Drijfhout, S. S., Fedorov, A. V., Hu, A., Jackson, L. C., Liu, W., McDonagh, E. L., Mecking, J. V., and Zhang, J.: Stability of the Atlantic Meridional Overturning Circulation: a review and synthesis, Journal of Geophysical Research: Oceans, 124, 5336–5375, https://doi.org/10.1029/2019JC015083, 2019.

Zhang, R., Sun, S., Chen, Z., Yang, H., and Wu, L.: On the decadal and multidecadal variability of the Agulhas Current, Journal of Physical

690 Oceanography, 53, 1011–1024, https://doi.org/10.1175/JPO-D-22-0123.1, 2023.